

Frauke Schulze · Jochen Kuss · Akmal Marzouk

Platform configuration, microfacies and cyclicities of the upper Albian to Turonian of west-central Jordan

Received: 6 October 2003 / Accepted: 6 October 2004 / Published online: 29 January 2005
© Springer-Verlag 2005

Abstract We present a comprehensive facies scheme for west-central Jordan platform deposits of upper Albian to Turonian age, discuss Cenomanian and Turonian carbonate cycles, and reconstruct the paleogeographic evolution of the platform. Comparisons with adjacent shelf areas (Israel, Sinai) emphasize local characteristics as well as the regional platform development. Platform deposits are subdivided into fifteen microfacies types that define eight environments of deposition of three facies belts. Main facies differences between Cenomanian and Turonian platforms are: rudist-bearing packstones that characterise the higher-energy shallow subtidal (transition zone) during the Cenomanian, and fossiliferous (commonly with diverse foraminifer assemblages) wackestones and packstones of an open shallow subtidal environment. On Turonian platforms high-energy environments are predominantly characterised by oolitic or bioclastic grainstones and packstones, whereas peritidal facies are indicated by dolomitic wackestones with thin, wavy (cryptmicrobial) lamination. Rhythmic facies changes define peritidal or subtidal shallowing-up carbonate cycles in several Cenomanian and Turonian platform intervals. Cyclicities are also analysed on the base of accommodation plots (Fischer Plots). High-frequency accommodation changes within lower Cenomanian cyclic bedded limestones of the central and southern area exhibit two major ‘cyclic sets’ (set I and II) each containing re-

gionally comparable peaks. Accommodation patterns within cyclic set II coincide with the sequence boundary zone of CeJo1. The lateral and vertical facies distributions on the inner shelf allow the reconstruction of paleogeographic conditions during five time intervals (Interval A to E). An increased subsidence is assumed for the central study area, locally (area of Wadi Al Karak) persisting from middle Cenomanian to middle Turonian times. In contrast, inversion and the development of a paleo-high have been postulated for an adjacent area (Wadi Mujib) during late Cenomanian to early Turonian times, while small-scale sub-basins with an occasionally dysoxic facies developed northwards and further south during this time interval. A connection between these structural elements in Jordan with basins and uplift areas in Egypt and Israel during equivalent time intervals is assumed. This emphasises the mostly concordant development of that Levant Platform segment.

Keywords Microfacies · Cyclicities · Paleogeography · Albian · Cenomanian-Turonian · West-central Jordan

Introduction

The microfacies of upper Albian to Turonian carbonate dominated deposits of Jordan was studied by (Al-Rifaiy and Cherif 1987), who considered considerable differences between Albian-Cenomanian and Turonian platforms. Powell (1989) presented a comprehensive outline of depositional environments and bathymetrical variations, concerning the entire investigated succession. Moreover, Al-Rifaiy et al. (1993) developed an environmental scheme for late Cretaceous times, including littoral to outer neritic depositional environments, Bandel and Geys (1985) described paleoenvironmental conditions for north Jordan, mainly based on echinoids, and Mustafa and Bandel (1992) described a lagoonal facies based on gastropods. Cyclic patterns within Cenomanian and Turonian platform deposits of the study area have rarely been mentioned by previous authors, except for

F. Schulze (✉) · J. Kuss
Department of Geosciences,
University of Bremen,
P.O. Box 33 04 40, 28334 Bremen, Germany
e-mail: frauke.schulze@neftex.com
Tel.: ++44(0)1235-443-627
Fax: ++44(0)1235-443-629

Present address:

F. Schulze, Neflex Petroleum Consultants Ltd,
71, Milton Park, Abingdon, Oxon, OX14 4RX, UK

A. Marzouk
Geology Department, Faculty of Science,
Tanta University,
Cairo, Egypt

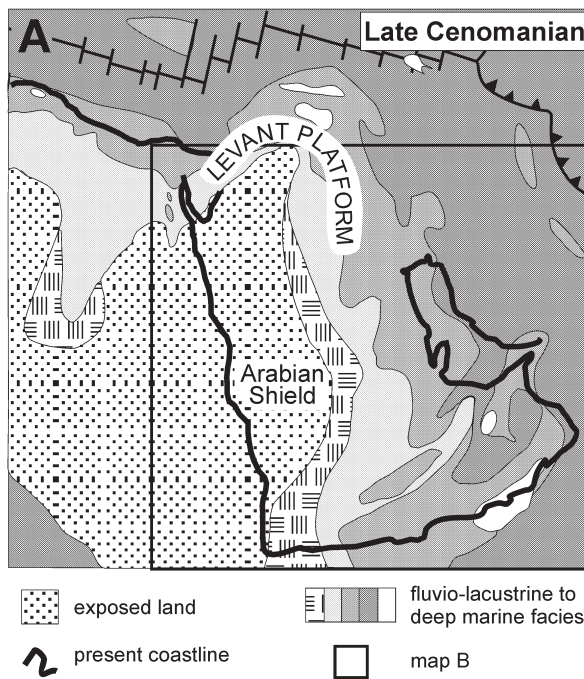
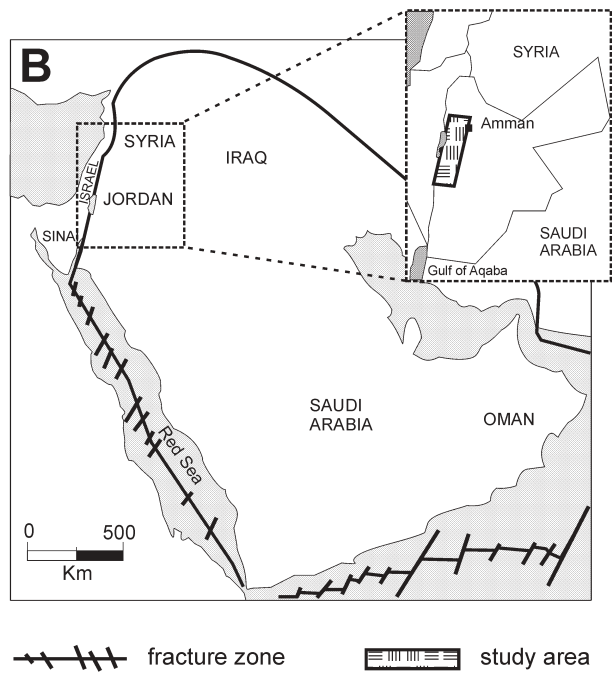


Fig. 1 a Paleogeographic map (after Philip et al. 2000) illustrates the distribution of facies belts on the Arabian Peninsula and indicates the position of the Levant Platform which contains the Cenomanian and Turonian platforms of Jordan and adjacent areas.



b The map after Sharland et al. (2001) gives an overview to the Arabian Peninsula and shows the position of the study area in Jordan (inlay map)

Powell (1989) who identified 'upward-shallowing sequences' within limestone and dolostone units of the Naur Formation (members 'b' and 'd'). Our new facies interpretations include a classification of carbonates and microfacies types, as well as spatial and temporal reconstructions of depositional environments. Moreover, comparisons with a facies scheme of adjacent Sinai highlight similarities and differences on this broad shallow shelf system. The interpretation of carbonate cycles and accommodation changes on upper Albian-Cenomanian/Turonian platforms presented herein mainly follows the methods and considerations of Fischer (1964), Goldhammer et al. (1993), Sadler et al. (1993), Boss and Rasmussen (1995), and Grötsch (1996). We discuss the use of accommodation plots with respect to: (1) whether accommodation changes can be interpreted as sea-level variations; (2) whether these plots are a helpful tool to enhance sequence stratigraphic analyses and correlations; (3) whether accommodation changes are orbitally forced and eustatic. A sequence stratigraphic scheme for west-central Jordan has already been presented by Schulze et al. (2003). Cenomanian to Turonian platform development and sequence stratigraphic models of adjacent areas were described by Bachmann and Kuss (1998) and Bauer et al. (2002) from Egypt, and by Lipson-Benitah et al. (1990) and Buchbinder et al. (2000) from carbonate platforms/ramps in Israel.

Geological framework

Paleogeographic reconstructions for the Arabian Shield by Philip et al. (2000) and Stampfli et al. (2001) show that, during late Albian to Turonian times, the study area was part of the Levant Platform (Kuss et al. 2003), a broad shelf system, situated on the passive margin of the Arabo-Nubian Shield and influenced by the southern Tethys (Fig. 1a). During Aptian/Albian times, the shoreline crossed south-east Jordan, marked by prevailing peritidal to shallow subtidal platform environments and by southward increasing siliciclastics. Then, the shoreline shifted southward, coeval with a major transgression of the Tethys ocean (Powell 1989; Stampfli et al. 2001). Siltstones and sandstones prograded during sea-level lowstands. Limestones and dolostones of Cenomanian and Turonian age exhibit rhythmic facies changes. Shales and limestones that are rich in organic carbon formed in intraplateau central sections during middle Cenomanian times and in single localities of the entire study area during the Cenomanian/Turonian-boundary interval. Similar to the adjacent shelf areas of Israel (Lipson-Benitah et al. 1990; Buchbinder et al. 2000) and Sinai/Egypt (Kuss et al. 2000; Bauer et al. 2001; Fig. 1b), the studied shelf of west-central Jordan was structured by paleo-highs and depressions since middle Cenomanian times. This paleo-relief and the resulting bathymetrical variability are reflected by north to south facies changes, varying thicknesses, and lithological differences. Limestones and dolostones of Cenomanian and Turonian age exhibit rhythmic facies changes that define sedimentary

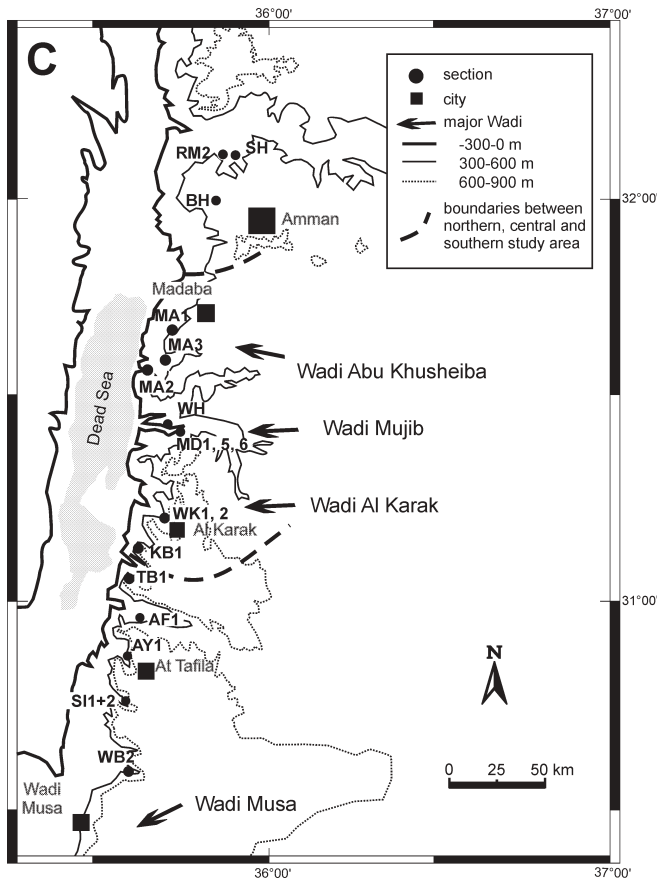


Fig. 2 Enlarged map of the study area; abbreviations of sections/localities: *SH* Salhub, *RM* Rumaymin, *BH* Bahhath, *MA* Wadi Abu Khusheiba, *WH* Wadi Al Hidan, *MD* Mujib Dam, *WK* Wadi Al Karak, *KB* Kuthrubba, *TB* At Talibbiya, *AF* Afra Springs, *AY* Ayma, *SI* Silla, *WB* Wadi Bustani

sequences of different order. Shales and limestones that are rich in organic carbon formed in central sections during middle Cenomanian times and in single localities of the entire study area during the Cenomanian/Turonian-boundary interval. Both ‘events’ are discussed in context with global transgressions, and anoxic events (OAE 2; compare, e.g., Arthur et al. 1987).

Methods

Detailed sedimentologic and palaeontologic investigations have been carried out on 18 sections throughout the study area (Fig. 2). Limestones and dolostones have been investigated using thin sections, while the carbonate classification followed the scheme of Dunham (1962) which comprises mudstones (ms), wackestones (ws), packstones (ps) and grainstones (gs). Semiquantitative estimations (0 = absent; 1 very rare = <10%; 2 rare = <20%; 3 common = <40%; 4 abundant = >40%) after Bacelle and Bosellini (1965) allow to determine main and accompanying components. Moreover, microfacies and facies analyses are based on investigation schemes of

Folk (1962), Wilson (1975) and Flügel (1982). The sequence stratigraphic concept follows Van Wagoner et al. (1988) and Vail et al. (1991). Indicative surfaces, like hardgrounds, and drowning surfaces, have been considered as sequence boundaries (SBs). The latter have been numbered according to Hardenbol et al. (1998), e.g., sequence boundary CeJo1: Ce = Cenomanian, Jo = Jordan, 1 = first SB in the Cenomanian. Investigations of higher-frequency cycles follow the model of Fischer (1964). Their interpretation as accommodation plots follows Tucker and Wright (1990), Strasser (1991), Burchette and Wright (1992), Goldhammer et al. (1993), Sadler et al. (1993), and Grötsch (1996). Enveloping curves of accommodation plots are created by graphic correlation.

Stratigraphy

Lithostratigraphy

The investigated upper Albian to Turonian succession of west-central Jordan (Fig. 2) is referred to the Ajlun Group (Quennell 1951), which overlies siliciclastics of the lower Cretaceous Kurnub Group, and comprises, after Masri (1963), the following five formations: Naur Limestone (NL), Fuheis (F), Hummar (H), Shueib (S) and Wadi As Sir Limestone (WSL, Fig. 3). The Ajlun Group is overlain by upper Coniacian-Santonian chalks and marls of the Belqa Group (Powell 1989).

Parts of the Naur Formation (members b and d; Fig. 3), the entire Hummar Formation and the Wadi As Sir Formation, predominantly consist of cliff-forming, dolomitic limestones and dolostones. In contrast, deposits of the Fuheis and Shueib formations mainly consist of marls or clays and form moderate slopes between the limestone cliffs (Fig. 3). In the central and southern parts of the study area, the lithological differences between the formations are less obvious. Massive limestones and dolostones of the Hummar Formation decrease in thickness from north to south. They interfinger with an intercalation of marls/clays with thin limestone beds in some sections south of Wadi Mujib (Fig. 2). Therefore, Powell (1989) defined the ‘F/H/S undifferentiated’ Formation. However, a subdivision of the five formations within the entire study area is possible, based on a new stratigraphic scheme (Schulze et al. 2003, 2004). These lateral variations result from a general shallowing towards the south and increasing terrigenous input within the proximal areas. A comprehensive description of the mentioned formations is given by Powell (1989) and Schulze et al. (2003).

Biostratigraphy

The biostratigraphic framework of the investigated succession is mainly based on ammonites and calcareous nannofossils. Additionally, benthic and planktic for-

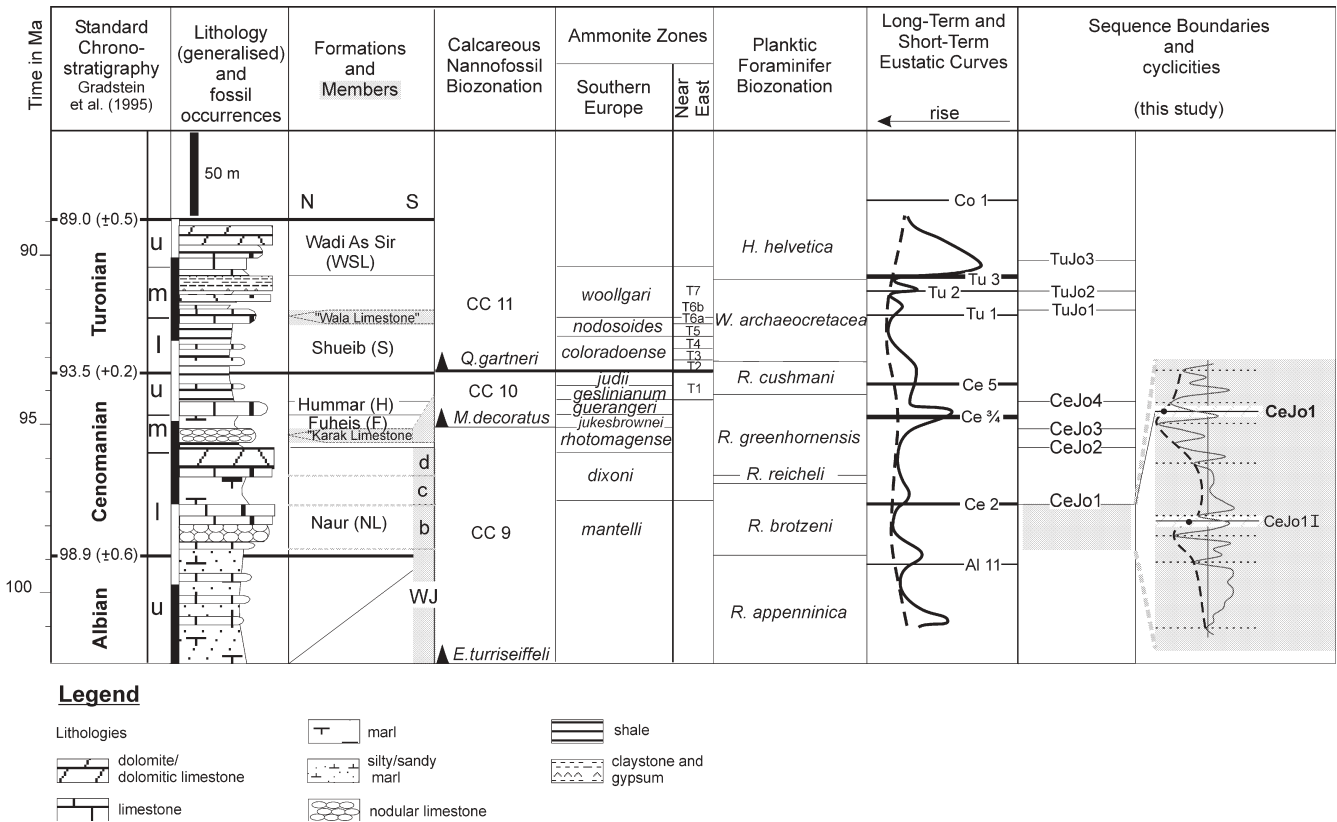


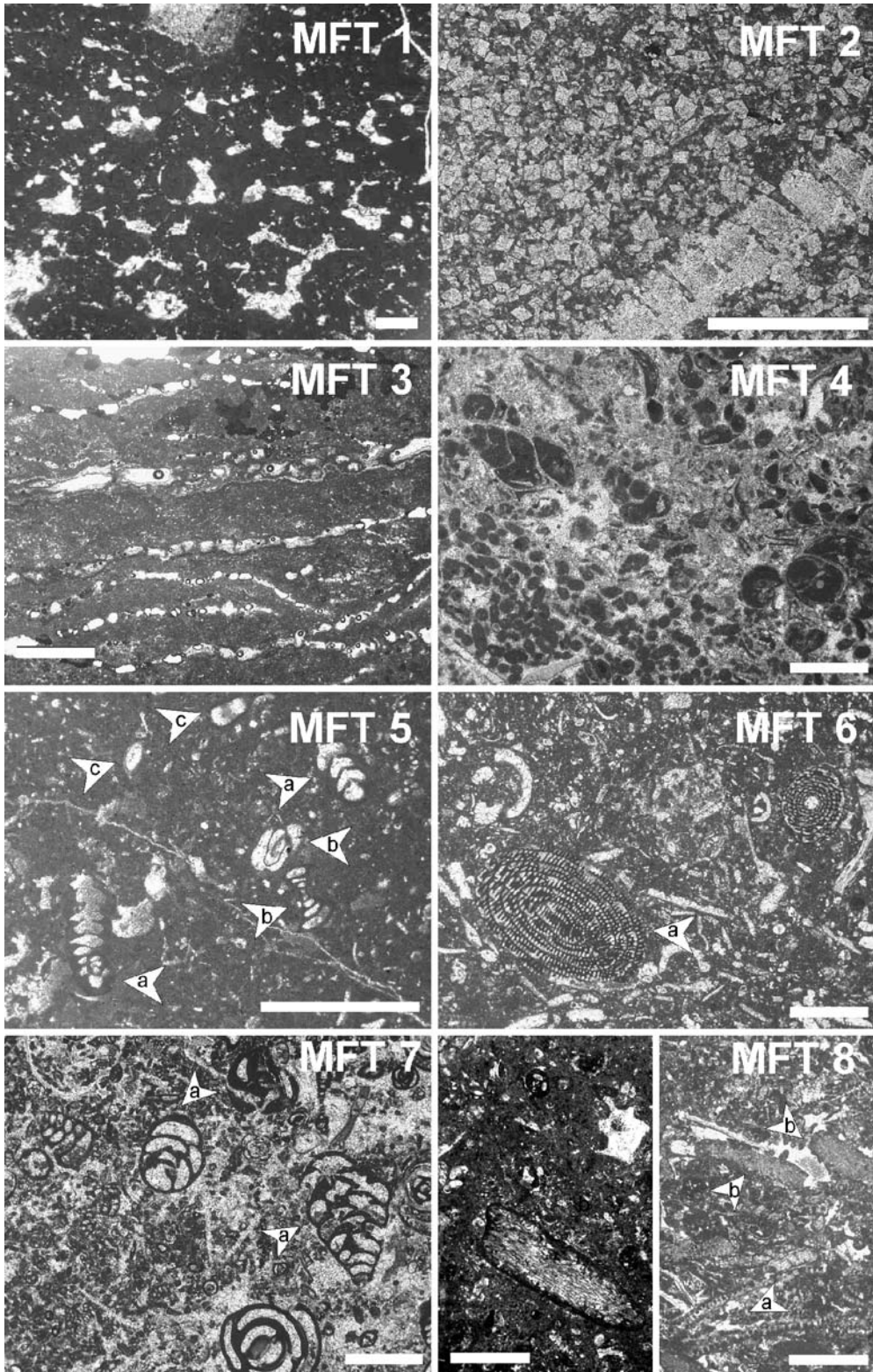
Fig. 3 A multi-stratigraphic framework of the upper Albian to Turonian succession in west-central Jordan (after Schulze et al. 2003) is compared to the time scale of Gradstein et al. (1995; left side). The established sequence boundaries are mentioned in the

right hand side column together with an example of an accommodation plot (Fischer Plot; grey box) resulting from higher-frequency cyclicities of lower Cenomanian carbonates (Naur Formation, Member b)

aminifers as well as ostracodes have been used for age determinations (Fig. 3; Schulze et al. 2004).

Ammonites have been identified by Z. Lewy (Geological Survey, Jerusalem/Israel). We followed the ammonite zonation of Southern Europe (Hardenbol et al. 1998) and Israel (Freund and Raab 1969; Lewy 1989, 1990). Specimens from the *mantelli* to the *woollgari* Zones allow subdivision of the lower Cenomanian to middle Turonian deposits. The nannoplankton is moderately preserved and exhibits a varying abundance. Calcareous nannofossils have been determined by A. Marzouk (Tanta University Cairo/Egypt), following Sissingh (1977) and Perch-Nielsen (1985). Compared to the biochronozones of the Tethyan realm according to von Salis in Hardenbol et al. (1998), the biozones CC 9, CC 10 and CC 11 have been subdivided based on the first occurrences of *Eiffelithus turriseiffelii*, *Microrhabdulus decoratus* and *Quadrum gartneri*. Benthic foraminifers have been studied in thin-sections and in washed residue of marl and clay samples, and they are mainly classified after Hamaoui and Saint-Marc (1970), Saint-Marc (1974), Schröder and Neumann (1985), Weidich and Al-Harithi (1990), Koch (1968), and Al-Rifaiy et al. (1993). Some larger foraminifers are biostratigraphically indicative and enable subdivision of the Cenomanian succession (compare Schulze et al. 2003; 2004). Planktic foraminifers

Fig. 4 Thin section photographs, showing characteristic component distributions and textures of eight microfacies types (MFT 1–8). All scale bars are equivalent to 100 µm. Abbreviations: *ms* mudstone, *ws* wackestone, *ps* packstone, *gs* grainstone. **MFT 1:** *ms* with fenestral structures; pores with triangular or irregular shape are filled with spar cement; Wadi Abu Kusheiba, section MA2 (lower Cenomanian, Naur Formation). **MFT 2:** dolomite or dolomitic *ms*; dolomite rhombs (occasionally zoned), rare shell fragments; Wadi Mujib, section WM3 (Turonian, Wadi As Sir Formation). **MFT 3:** *ms* with wavy lamination (microbial layers); primary pores filled with spar cement, section MD1 (middle Cenomanian, Fuheis Formation). **MFT 4:** *ws/ps* with abundant gastropods and peloids; strongly bioturbated, faecal pellets concentrated in nests; Wadi Abu Kusheiba, section KU3 (Turonian, Wadi As Sir Formation). **MFT 5:** *ms/ws* with low diversity benthic foraminifers; agglutinated forms and miliolids prevail, ostracodes, fragments of echinoids and non-differentiable bioclastic components are common; (a) *Pseudorhapydionina dubia*; (b) miliolids, (c) ostracodes; Rumaymin, section RM2 (lower Cenomanian, Naur Formation). **MFT 6:** *ws/ps* with larger alveolinid foraminifers; fragments of calcareous green algae, benthic and planktic foraminifers and bioclasts are associated; (a) *Praealveolina cretacea*; Wadi Al Karak, section WK2 (middle Cenomanian, Naur Formation). **MFT 7:** *ws/ps* with benthic foraminifers (high diversity); characteristic form is *Chrysalidina gradata* (a), abundant peloids and bioclasts are associated, moderate to strong bioturbation and/or winnowing; Rumaymin, section RM2 (lower Cenomanian, Naur Formation). **MFT 8:** *ws/ps* with calcareous green algae; bioclasts, echinoid fragments, benthic and planktic foraminifers; matrix is predominantly micritic and slightly reworked; (a) Udoteacea, (b) Dasycladacea; sections of two thin sections are presented: left side: At Talibbiya, section TB1 (lower Cenomanian, Naur Formation); right side: Wadi Mujib, section MD6 (Turonian, Wadi As Sir Formation)



have been identified after Caron (1985). First occurrences of *Heterohelix globulosa* (= *H. reussi*; Nederbragt 1991), *Whiteinella aprica* and *W. archaeocretacea* (W. Kuhnt, oral com., 2001) indicate the uppermost Cenomanian to lower Turonian (*W. archaeocretacea* and *R. cushmani* Biozones, Fig. 3). M. A. A. Bassiouni and A.-M. M. Morsi (both Ain Shams University, Cairo/Egypt) have identified a relatively diverse ostracode fauna. Indicative species allow to subdivide the Cenomanian deposits (compare also Morsi and Bauer 2001). Moreover, deposits of the CT-boundary interval (upper Cenomanian/lower Turonian) are distinguishable from late Turonian successions.

Sequence stratigraphy

Seven sequence boundaries (SB's) define eight sedimentary sequences for the study area. Four SB's are within the Cenomanian succession (CeJo1-4) and three within the Turonian one (TuJo1-3; Fig. 3). The SB's are either developed as distinct surfaces marked by iron crusts and vertical borings, or as boundaries separating deposits of a sea-level highstand (HST) from a sea-level lowstand (LST) succession. Those are indicated by clear facies changes, e.g., shallow subtidal/intertidal limestones overlain by supratidal siliciclastics. Indicators for transgression are, e.g., reworking patterns or a sharp transition from shallow-water limestones or dolostones to deeper-water marls or shales above a transgressive surface. At some positions on the shallow platform, where carbonate production exceed the increase of accommodation space, aggrading carbonate successions developed during transgressive phases ('keep-up' system after Sarg 1988; Pasquier and Strasser 1997). An early sea-level highstand is mainly characterised by progradation of limestones or clays that contain abundant ammonites and planktic foraminifers and reflect open, deep subtidal facies. During late HST's, aggradation of thick dolostone or limestone units, deposited in shallow subtidal to peritidal environments occur. These HST carbonates commonly exhibit rhythmic shallowing-up patterns of different scale. Sea-level lowstand deposits of middle Cenomanian times occur in the central study area (Wadi Mujib, Wadi Al Karak; Fig. 2) and are represented by peritidal (mudstones with monotypic ostracodes or microbial lamination) and agitated shallow subtidal environments (rudist 'patch reefs'). A major middle Turonian LST can be traced over the entire investigated platform. It is represented by dolomites in northern sections, while greenish and reddish claystones and gypsum beds mark this lowstand in most central sections. Evaporites interfinger with siltstones and sandstones in the southern study area. Furthermore, transgressions of the middle Cenomanian and the Cenomanian/Turonian-boundary interval are locally reflected by a restricted deep subtidal and occasionally dysoxic facies. A comprehensive description of the sequence-stratigraphic model is given in Schulze et al. (2003).

Results

Microfacies

The most abundant and most indicative components are subdivided according to whether they have a biogenic (skeletal) or an abiogenic (non-skeletal) origin. Based on these investigations, fifteen microfacies types (MFTs) are defined (Figs. 4 and 5) that are assigned to eight environments of deposition.

Skeletal components

The most frequent skeletal components of the investigated limestones are shells and test fragments of gastropods, different bivalves (often oysters), ostracodes, foraminifers and calcareous green algae. Fragments of echinoids, spiculae (sponges) and undifferentiated bioclasts also occur abundantly. Rudists, corals or bryozoans are rarely observed.

Rudist fragments (Fig. 5, MFT 9) indicate deposition in a higher-energy environment, at or close to small rudist 'patch reefs'. Fragments of Rhodophyta ('red algae') are often associated with Udoteacea (green calcareous algae; Fig. 4, MFT 8) also prevail in higher-energy environments. The same is true for thick-shelled oysters that may also grow in 'patch reef'-like structures. Associations of benthic foraminifers that are dominated by larger agglutinated forms (e.g., orbitolinids) suggest increased water energy and also probably an increased siliciclastic input. Moreover, broken shells or tests indicate higher wave energy (very shallow environments; storms) or transport

Fig. 5 Thin section photographs, showing characteristic component distributions and textures of microfacies type 9 to 15. Abbreviations: see Fig. 4; all *scale bars* are equivalent to 100 μm . *MFT 9*: ps with rudist fragments; diverse other biogenic components (e.g., algae, foraminifers, bivalves; mostly well- or sub-rounded), peloids, and coated grains, moderate winnowing; arrows indicate rudist fragments; Silla, section S11 (lower Cenomanian, Naur Formation). *MFT 10*: ws/ps with algal debris; undefined bioclasts, filaments, and planktic foraminifers are associated, micritic matrix; Kuthrubba, section KB1 (lower Cenomanian, Naur Formation). *MFT 11*: ps/gs with large shell fragments; bivalves dominate; gastropods, ostracodes, and extraclasts also occur, commonly with poor sorting; Wadi Al Karak, section GM1 (middle Turonian, Shueib Formation). *MFT 12*: ps with ooids (mostly superficial); other coated grains, peloids, intraclasts, extraclasts, and ostracodes are associated, moderate to intensive winnowing, (a) quartz grains (subrounded, rounded), arrows indicate ooids; Wadi Abu Kusheiba, section KU2 (Turonian, Shueib Formation). *MFT 13*: gs with ooids; normal ooids may be associated with other coated grains, intraclasts, and bioclasts, components are mostly well-sorted; Wadi Mujib, section MD6 (Turonian, Wadi As Sir Formation). *MFT 14*: ms with organic material; organic material, phosphate and planktic foraminifers are often concentrated in thin laminae; Wadi Al Karak, section WK2 (upper Cenomanian, Shueib Formation). *MFT 15*: ms/ ws with planktic foraminifers; calcispheres may be associated, planktic foraminifers consists of globular forms, (a) *Hedbergella* spp., (b) *Heterohelix* spp., dark patches of organic or phosphatic material occasionally occur; Salhub, section SH1 (upper Cenomanian, Shueib Formation)

by currents. In contrast to these higher-energy indicators, abundant gastropod tests and high amounts of thin-shelled miliolids (Fig. 4, MFT 5) or other opportunistic benthic foraminifers occur in low-energy (lagoonal) regimes. Indicators for open, deeper-water environments are high amounts of entire tests of planktic foraminifers (Fig. 5, MFT 15). Abundant calcispheres, spiculae or ammonites also indicate deeper-water and fully marine conditions. In contrast, microbial laminae (Fig. 4, MFT 3) reflect very shallow-water conditions in peritidal environments. Moreover, some biogenic components characterise 'stress' conditions within restricted environments. Miliolid-dominated benthic foraminifer assemblages, e.g., reflect decreased circulation and probably reduced oxygen contents or euryhaline conditions. High amounts of monotypic ostracodes are interpreted as indicators for very shallow environments, and occasional fresh water input can be assumed. A co-occurrence of abundant gastropods and small fecal pellets (enriched in clusters; after Flügel 1982; Fig. 4, MFT 4) and strong bioturbation imply a shallow, low-energy environment. Abundant larger and structured coprolites of the benthic macrofauna (e.g. Crustaceans) reflect after Senowbari-Daryan and Kuss (1992) decreased oxygen contents and occasionally fresh water influence. In contrast, a well-lit and oxygenated shallow subtidal environment is reflected by a highly diverse benthic assemblage of, e.g., calcareous green algae and benthic foraminifers, accompanied by e.g. fragments of echinoids, corals, bivalves and planktic foraminifers (Figs. 4 and 5; MFT 6, 7, 8, 10).

Non-skeletal components

Coated grains, peloids, and intraclasts occur abundantly, while oncoids, ooids, and extraclasts are subordinate. Please mention that we defined all grains with a micritic envelope as 'coated grain', without a subdivision of a destructive or constructive origin of the envelope. Two types of coats were observed: (a) one or more dark, micritic layer, partly with enriched organic material or small components (skeletal debris). The layer-surfaces are often undulated. These coats are interpreted as constructively built by micro-organisms. From a certain point there is a smooth transition towards oncoids (see below), (b) coated grains with envelopes that are destructively generated by boring micro-organisms seem to dominate. Following the definition of Flügel (1982) and Bathurst (1966) both types are used as low energy indicators in shallow-water environments. Peloids indicate moderate reworking by bottom currents or wave activities. Increased water energy can also be assumed, if abundant intraclasts occur. Extraclasts mainly consist of components of adjacent inner shelf environments, but detrital quartz grains also belong to this group. Both imply transport by bottom currents and/or transport by sliding into relatively deeper water areas. Consequently, extraclasts reflect higher-energy conditions (transition zone), partly continental input and a certain structuring of the inner shelf (Fig. 5, MFT 12). Observed

ooids dominantly show tangential structures. Normal ooids with several laminae commonly occur and indicate high-energy environments (Flügel 1982; Fig. 5, MFT 13). Tangential ooids are also described from hypersaline environments (Garber et al. 1981), but the co-occurring biotas do not confirm this interpretation within the investigated samples. Few superficial ooids with one or only few laminae occur. These ooids occur together with peloids and rare intraclasts. They imply a lower water-energy than normal ooids do (transition zone). The differentiation of superficial ooids and coated grains was not always possible. Microbial or algal oncoids (Flügel 1982) are observed. They indicate shallow-water and lower-energy conditions of lagoonal or transition zone areas. Glauconite grains (often well rounded) abundantly occur together with gastropods or ostracodes. Glauconite is also rarely observed as filling of ostracode or foraminifer shells. Within these associations, components with micritic envelopes, microbial crusts and a strong bioturbation are additionally observed. Phosphatic material is represented by phosphate pellets, fish teeth or other fish remains.

Textures and structures

Limestone textures indicate syndepositional and post-depositional mechanisms. Different types of lamination were observed. Wavy lamination consists of irregular, wavy, micritic horizons (algal laminae) with probably primary interlamellar interspaces (after Flügel 1982) and intercalated silty layers (Fig. 4, MFT 3). Washover from the open, shallow subtidal, such as single chambers of planktic foraminifers, is enriched in single horizons. Restricted, shallow subtidal to peritidal environments (e.g. tidal flats) are reflected. Common thin lamination contains regular micritic layers. Organic material and abundant planktic foraminifer tests are enriched in single layers. Benthic organisms or bioturbation fabrics rarely occur, except nearly monospecific, opportunistic benthic foraminifers and/or smooth-shelled ostracodes. This points to a restricted, oxygen depleted environment and probably deeper-water conditions (Fig. 5, MFT 14). Among the fenestral fabrics in a micritic matrix, the 'stromatactics'-type dominate. The open-space structures mainly have a triangular shape and are filled with sparite. Stromatactics point to deposition in peritidal (mainly supratidal) environments (Fig. 4, MFT 1). Washed-out micritic matrix in packstones or grainstones, which is replaced by sparitic cements ('winnowing' after Flügel 1982; Fig. 5, MFT 13) implies increased wave or current energy. These conditions are characteristic for high-energetic environments, such as sandbars or shoals in the shallow subtidal belt. Winnowing also occurs in beach sediments (intertidal). Moreover, bioturbation strongly affected the intertidal to shallow subtidal deposits: the original textures and grain-size distributions are disturbed or destroyed. A mottled structure or circularly arranged bioclasts are characteristic bioturbation fabrics. Well

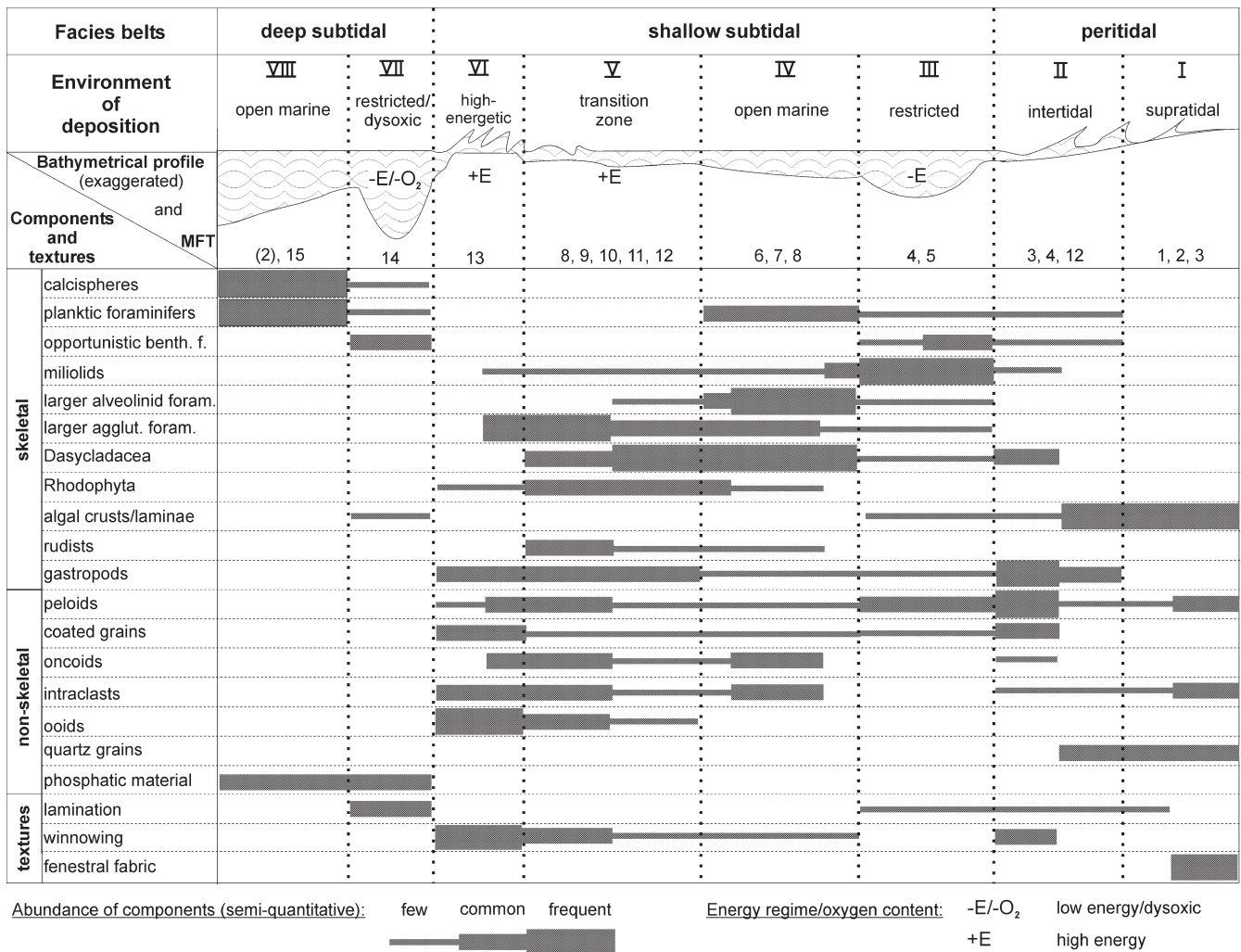


Fig. 6 Semi-quantitative abundance and distribution of skeletal and non-skeletal components, and limestone textures within the eight environments of deposition (I–VIII) are illustrated. The environments are assigned to three facies belts on the inner shelf (peritidal to deep subtidal). The bathymetrical profile shows the occurrences

of the 15 microfacies types (see Figs. 4 and 5), topographic differences on the inner shelf and characterising facies conditions for the environments. For schematic reasons, the bathymetric profile across the depositional environments is exaggerated

sorted and rounded components additionally imply higher water energy, or at least, recurring reworking and transport (Fig. 5, MFT 12, 13). Discontinuities or interruptions in 'normal' sedimentation frequently occur. Different kinds of surfaces were observed. Hardgrounds occur often on top of small-scaled shallowing-up sedimentary sequences with peritidal dolomites in the upper part (Fig. 4, MFT 2). Ferruginous crusts and vertical borings reflect a sedimentary break. Another type of discontinuity surfaces are condensation horizons. These were rarely observed on top of deeper water successions. Poorly sorted and partly poorly rounded components occur densely packed. Phosphatic, organic and glauconitic grains/ material are enriched in single layers. The surface is often represented by hard ferruginous crusts (Fig. 5, MFT 11).

Environments of deposition

Based on the microfacies investigations eight environments of deposition belonging to three major facies belts are identified (Figs. 6 and 7).

Peritidal facies belt

Peritidal facies belts include intertidal and supratidal environments of deposition, influenced by permanent submergence and emersion. Supratidal zones are regularly affected by spring tides or storm events. Stressed conditions, like high salinity, persistent reworking or occasionally high sedimentation rates (storms, input from the continent) are reflected by e.g. microbial crusts, a non-diverse fauna (gastropods, ostracodes), peloids, quartz grains, dolomite and fenestrae. These components and

West Central Jordan
(this study)

Sinai / Egypt
(Bauer et al., 2003)

Environment of deposition	Microfacies Type (MFT)	Legend	MFT	Facies belt		
peritidal	I supratidal ms + fenestral fabric	III, 4 environment, microfacies type which occur in both study areas VII, 14 environment, microfacies type which occur only in one study area	S1	siliciclastic shoreface		
	II intertidal dolomite					
shallow subtidal	III restricted lagoon ms + algae laminae (+ ostracodes)	+E high energy -E low energy -O₂ low oxygen content	L1	lagoon		
	IV open marine ws/ps + gastropods (+ peloids, fecal pellets/coprolithes)				L2	
	V transition zone ms/ws + low diverse benthic foram. (+ echinoids/ostracodes)				L3	
	VI high-energetic ws/ps + larger alveolinid foraminifers (+ calcareous algae)		VI, 14 environment, microfacies type which occur only in one study area	+E high energy -E low energy -O₂ low oxygen content	P1	shallow subtidal
	VII restr. / dysox ws/ps + benthic foraminifers (high diverse assemblages)				P2	
	VIII open marine ws/ps + calcareous algae (+ planktic foraminifers)				P3	
	IX high-energetic ps + rudists (+ algal debris, planktic foraminifers)				P4	
	X high-energetic ws/ps + algal debris (planktic f.)		VI, 14 environment, microfacies type which occur only in one study area	+E high energy -E low energy -O₂ low oxygen content	P5	high-energy subtidal
	XI high-energetic ps/gs + bivalves (+ gastropods, extraclasts)				W1	
	XII high-energetic ps + ooids/intraclasts/peloids/oncooids				W2	
XIII high-energetic gs + ooids/intraclasts/bioclasts	W3					
deep subtidal	XIV restr. / dysox laminated ms (phosphate, opportunistic f./planktic foraminifers)	VI, 14 environment, microfacies type which occur only in one study area	W4	deep water		
XV open marine ms/ws + planktic foraminifers, calcispheres	B1					

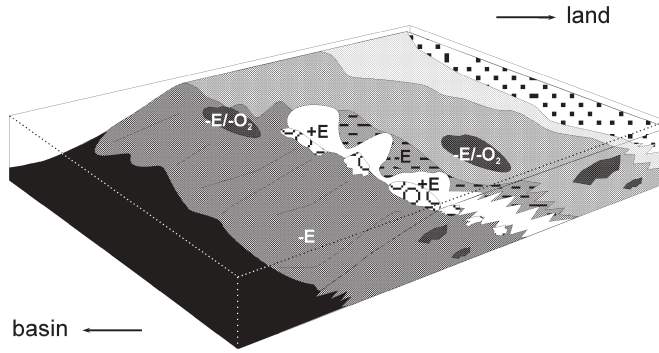


Fig. 7 Microfacies types (MFTs) and facies belts of Jordan (left column) and Sinai/ Egypt (right column) are compared, while the MFTs of this study are briefly characterised. MFTs and environments that are congruent in both schemes are marked bold and

black. Differences are highlighted in grey. The block diagram illustrates all mentioned facies belts on the shelf (compare environments of deposition I–VIII, Fig. 6)

textures characterise the first four microfacies types (MFT 1–4; Figs. 6 and 7) and mainly point to deposition in tidal flats or ‘ponds’.

Shallow subtidal facies belt

The shallow subtidal facies belt includes four environments of deposition. Most microfacies types occur there (MFT 4–13, Figs. 6 and 7).

Restricted shallow subtidal environments of deposition are characterised by low-diversity ostracode, benthic foraminifer, or gastropod assemblages. The foraminiferal associations are commonly dominated by miliolids (MFTs 4, 5; Figs. 6 and 7). Thus, environments with unfavourable life conditions for many benthic organisms are indicated and a fluctuating salinity and/or decreased oxygen content can be assumed. Bioclasts (e.g. larger benthic foraminifers, echinoids) of nearby open subtidal environments co-occur. The clasts are commonly rounded and micritised.

Open marine shallow subtidal environments are characterised by microfacies types that include abundant and highly diverse faunal associations of calcareous green algae and benthic foraminifers, associated with rudists, corals, gastropods and planktic foraminifers (MFTs 6–8, Figs. 6 and 7). Diversity and intensive bioturbation reflect well-lit water and normal salinities and oxygen contents within the water column, at the sediment surface and

within the upper sediment layer. Abundant peloids and intraclasts additionally indicate increased water energy, compared to the restricted environments.

A transition zone is evidenced by higher-energy indicators like abundant larger agglutinated foraminifers, red algae, rudists, intraclasts or few ooids and textures resulting from winnowing (MFT 8–12, Figs. 6 and 7).

High-energy shallow subtidal environments, like shoals or flat ‘patch reefs’, are indicated by wave agitated, winnowed deposits that mostly contain ooids, bioclasts (oysters, rudists), intraclasts (MFT 13, Figs. 6 and 7).

Deep subtidal facies belt

Deep subtidal facies belts include restricted and open marine deeper-water environments.

A restricted deep subtidal area of deposition with occasionally dysoxic conditions is characterised by thin lamination with enriched phosphatic and organic material. Either abundant calcispheres/planktic foraminifers or assemblages of small opportunistic benthic foraminifers (e.g. buliminids, MFT 14; Figs. 6 and 7) additionally occur. Although, planktic fauna and flora is partly enriched, they do not imply hemipelagic or pelagic conditions.

Open marine deep subtidal environments are indicated by high amounts of well-preserved planktic foraminifers, calcispheres or ammonites (MFT 15, Figs. 6 and 7).

Phosphate grains or phosphatic fish remains may also occur. Dolostones that exhibit a lack of components and textures may also be assigned to this facies belt (Fig. 6, MFT 2).

Comparison with Sinai/Egypt

A comparison of microfacies types and depositional environments of this study with the facies models of the adjacent shelf area of Sinai (Bauer et al. 2003; Fig. 7) reveals many analogies, but also some differences. Bauer et al. (2003) divide the upper Cenomanian to Turonian inner shelf of Sinai into a deep-water facies belt, a subtidal facies belt, and a siliciclastic shoreface, while the subtidal is subdivided into high-energy, open shallow and restricted (lagoonal) environments. This subdivision mainly corresponds to the environments described of this study (Figs. 6 and 7). However, the siliciclastic shoreface as the most proximal facies belt after Bauer et al. (2003) is indicated by high-energy deposits rich in quartz, ooids, and bioclasts (MFT S1, S2; Fig. 7). The present facies scheme does not contain such a quartz-dominated environment. Instead, the present scheme includes supratidal and intertidal environments like tidal flats or ponds that are indicated by MFTs 1–3 (Figs. 6 and 7). On the other hand, deeper-water environments characterised by a microfacies type of deep subtidal and restricted/dysoxic environments (MFT 14; Figs. 6 and 7) have no equivalent within the scheme of Bauer et al. (2003). These differences in platform organisation are discussed later.

Cyclicities

Cyclic shallowing-up sequences of dm- to m-scale are frequently observed in the Cenomanian and Turonian carbonates of several localities. Both the cliff-building members of the Naur Formation (members b and d) and the limestones and dolostones of the Wadi As Sir Formation contain rhythmic shallowing-up patterns in the entire study area, while comparable shallowing-up cycles within platform deposits of the Hummar Formation are restricted to the northern sections. Microfacies and facies investigations provide a detailed subdivision of the cyclic successions, expose facies changes through time and enable to reconstruct relative sea-level changes and sequence stratigraphic elements (Fig. 8). Sedimentary sequences of different scale show also different sequence stratigraphic elements. Small-scaled 'elementary sequences' (dm to m; compare Strasser et al. 1999) often comprise a transgressive surface at the base, upward shallowing subtidal to peritidal sediments and a sequence boundary (SB) on top. The latter is recognizable by a prominent surface, e.g., a bored hardground, ferruginous crust, or a reddish colour. The transgressive surfaces often directly overlie the sequence boundaries. This is e.g. caused by reworking and reflected by intraclast (reworking) horizons that overlie a bored hardground.

Larger-scaled sequences (few metres to tens of metres) often clearly reflect deepening and shallowing, with transgressive (TST), highstand (HST) and partly lowstand (LST) deposits. In that case, the SB can be defined at the base of the 'shallowest deposits' (Fig. 8). Maximum flooding surfaces are almost not recognizable within the investigated shallow-water limestones, but in larger-scaled sequences maximum flooding zones (MFZ) are observed (Fig. 8) by a facies of maximum flooding/strongest marine influence.

Cyclicities of Cenomanian and Turonian platform carbonates

The thickness of different-scale sedimentary sequences on both platforms varies between some centimetres and several metres, or tens of metres. The onset of a transgression is in Cenomanian carbonates mostly reflected by a sharp contact between peritidal limestones and marine, subtidal limestones with strong bioturbation. Transgression deposits on the Turonian platform are also composed of bioturbated, bioclastic limestones, but additionally horizons with reworked clasts and ooids occur and reflect flooding and reworking (e.g. MFTs 9–13; Fig. 6). While fossiliferous subtidal limestones commonly reflect a HST on the Cenomanian platform (e.g. MFTs 4, 6, 9; Fig. 6), thick peritidal dolomitic limestones and dolostones with thin/wavy lamination represent the Turonian equivalents (MFTs 2, 3, 5; Fig. 6). Locally, shoals composed of bioclasts or ooids occur instead (MFT 13; Fig. 6). Lowstand deposits (LST) are difficult to recognize, in Cenomanian platform carbonates and in the Turonian sequences as well. Intertidal or supratidal limestones and dolostones that contain a non-diverse fauna or fenestral fabrics (e.g. MFTs 1, 2, 5; Fig. 6) locally reflect a LST on the Cenomanian platform. The described Turonian peritidal limestones and dolostones may represent late HST and also LST deposits.

Accommodation plots

To verify lateral correlations and to provide sequence stratigraphic interpretations, the accommodation rates of the described cyclicities have been investigated, additionally to their facies characteristics. Cyclically bedded units of the Cenomanian to Turonian succession were measured in detail in several sections of the study area. Following the scheme of Sadler et al. (1993) and Strasser et al. (1999), the cycles were counted and the deviation of the mean cycle thickness was plotted. Cyclicities within the lower cliffs of the Naur Limestone Formation (member 'b'; Figs. 3 and 9) are illustrated and described based on four sections of the central and southern study area (WK1, TB1, AF1, SII+2; Figs. 2 and 10). The cyclically bedded successions of the same interval of the two sections AF1 and SII+2 (Fig. 9) contain different lithologies and sedimentary patterns. To provide a re-

producable definition of cycles, the facies succession (deep to shallow subtidal or subtidal to peritidal; compare e.g. Osleger 1991; Strasser et al. 1999) from the deepest to the shallowest part has been determined.

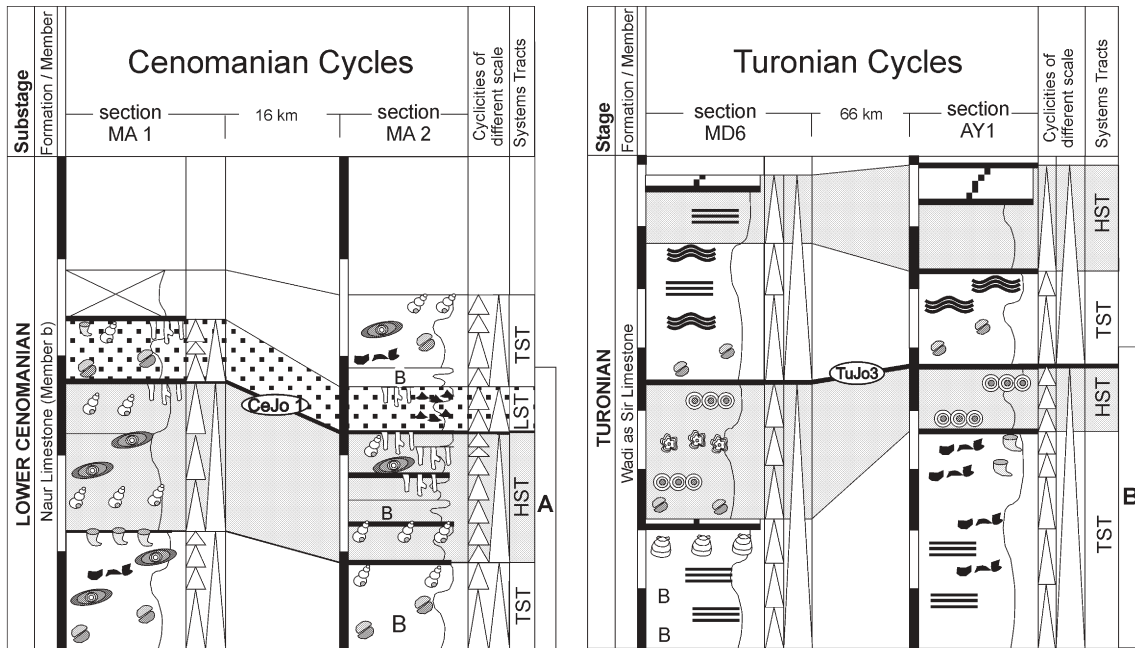
In section AF1, reworked layers (packstones with bioclasts, intraclasts or subrounded pebbles) indicate a transgressive phase; while massive, strongly bioturbated limestones mark the following relative sea-level highstand. The shallowest cycle-part is predominantly marked by platy, thinly laminated limestones and dolostones (Fig. 9). In contrast, the cyclic bedding of member b in section SII+2 (Fig. 9) is reflected by an upward thinning (compare Goldhammer et al. 1993), from about 30 cm thick beds at the base to 5 cm thick layers on top. Massive limestones or dolostones represent 'deep' cycle parts, while thin lamination and reworking patterns mark the shallower units. Cycles in section SII+2 are mostly topped by hardgrounds, iron-crusts, and vertical borings. These surfaces reflect the cycle boundaries. Cycles of both sections were counted and the deviation from the mean cycle thickness was plotted against the cycle number (Fig. 9). A positive divergence from the mean cycle thickness reflects higher accommodation rates, whereas negative deviations exhibit lower accommodation rates (e.g. Goldhammer et al. 1993). A comparison of both curves exhibits differences but also similar patterns, such as several positive peaks of accommodation rate and rhythmic divergences from the mean cycle thickness (Fig. 9). Correlation of these accommodation changes cannot be supported by biostratigraphic data. Therefore, the following comparisons of cyclic sedimentary sequences (Fig. 10) rely on graphic correlation and single sequence stratigraphic elements (ts, SB). Seven main peaks have been counted in the plots of Figs. 9 and 10 ('a-g'). Their correlation shows similarities concerning the accommodation patterns, but varying cycle numbers between these positive peaks. In general, the total cycle number decreases towards the south from 80 cycles in section WK1 to 31 cycles in section SII (Fig. 10a). To figure out a general trend and to apply the curves for comparison with other sections, enveloping curves have been graphically created (touching all 'positive peaks' on the left side of the curve; Fig. 10a). A second enveloping curve, also graphically created, visualises two main accommodation maxima and one minimum, corresponding to two major 'cyclic sets' (Fig. 10b). Both sets include four of the counted main accommodation peaks (peak a-d, set I; peak e-h, set II; Fig. 10b), and one inflexion point (behind positive maxima; Fig. 10b).

Discussion

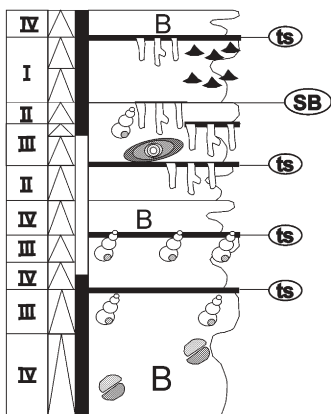
Lateral correlation of accommodation plots exhibits coincidences between major trends but also differences concerning the higher-frequency accommodation changes. Considering the discussion about use and interpretation of 'Fischer plots' (e.g. by Sadler et al. 1993; Boss and Rasmussen 1995; Grötsch 1996) possible errors and re-

strictions in the application of accommodation plots can be estimated. After Sadler et al. (1993), about 50 cycles are required for an accommodation plot to be representative. Lower numbers may produce errors that cannot be excluded for the studied accommodation plots, which are based on cycle numbers between 31 and 80. Furthermore, not all relative sea-level fluctuations are recorded on the shallow platform ('missing beats', e.g., Balog et al. 1997) and condensation and reworking may result in incomplete plots. The southward decrease of cycle numbers, mentioned above, is probably related to an amalgamation of cycles towards the continent. The completeness of cycles and a primary accommodation rate are, among others, the prerequisites for using 'Fischer Plots' as accommodation proxies. If 'Fischer Plots' are equivalent to accommodation plots, and if they can be interpreted as sea-level curves, is discussed by e.g. Boss and Rasmussen (1995). However, facies changes from deeper (e.g. subtidal) environments to a shallow (e.g. supratidal) facies reflect relative fluctuations of the water depth. Therefore, the single units of each cycle can be interpreted as systems tracts. The enveloping curves in Fig. 9b do not directly represent a superimposed trend of relative sea-level fluctuations, but aggrading cycles reflect a HST, thinning a falling sea level and thickening of cycles a sea-level rise. Therefore, we interpret the zone around the inflexion point within 'cyclic set II' to be associated with the sequence boundary-zone of SB CeJo1 (Fig. 10b). According to this, the flexure point-zone within cyclic set I may point to an additional SB within the lower Cenomanian Naur Formation (zone of CeJo1I, Fig. 10b). Peritidal shallowing-up cycles predominate within the investigated successions and imply after Ginsburg (1971), Goldhammer et al. (1993), Grötsch (1996) and Strasser et al. (1999) a successive filling of the available accommodation space within shallow subtidal areas. Carbonate production prevails in this case during a relative sea-level rise, and the shallowing is related to gradual progradation of tidal flat facies belts. Coevally, the carbonate production decreases, while subsidence persists. Thus, after a period of non-deposition, a deepening and an increasing productivity result and a new peritidal cycle begins (Ginsburg 1971; Strasser 1991; Pratt et al. 1992). These mechanisms cause the observed vertical facies changes and induce lateral shifts of facies belts. Cycles that contain a peritidal unit are commonly affected by erosion

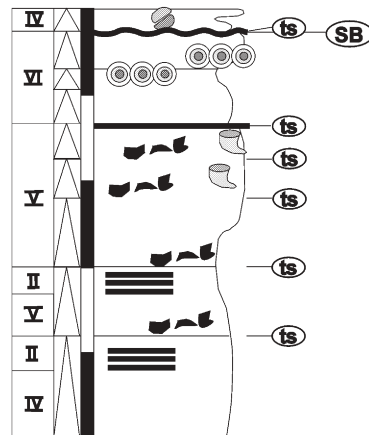
Fig. 8 Rhythmic facies changes and cyclic bedding of different scale within shallow-water carbonates are illustrated by Cenomanian and Turonian subsections. Transgressive sediments (TST), highstand deposits (HST) and the shallowest parts of the subsections (LST) are defined. Resulting sequence boundaries enable to correlate cyclic bedded successions. Cut-offs of the Cenomanian (a) and Turonian (b) rhythmic bedded carbonate successions show the connection between environmental changes (compare Fig. 6), small-scaled shallowing-up cycles, and sequence stratigraphic elements. Smallest distinguishable sedimentary sequences are between centimetres and several metres thick. These 'elementary sequences' are mainly separated by transgressive surfaces (ts) and sequence boundaries (SB)
















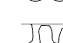









A CENOMANIAN

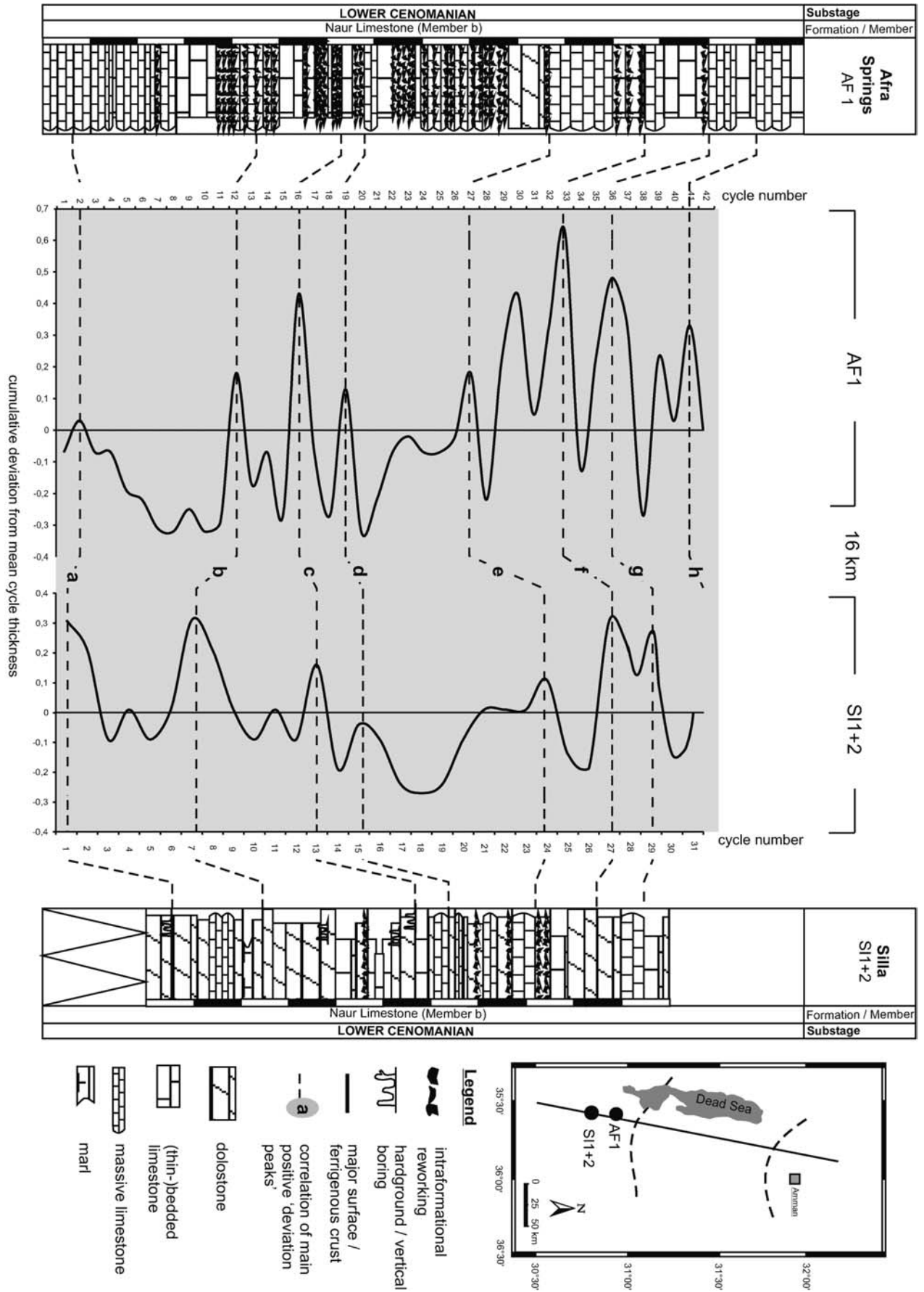


B TURONIAN



Legend

-  lowstand systems tract
-  highstand systems tract
-  transgressive systems tract
-  environment of deposition (see figure 6)
-  transgressive surface
-  'elementary sequence'
-  gastropods
-  rudist 'patch reef'
-  large benthic foraminifers
-  oyster 'patch reef'
-  strong bioturbation
-  oncoids
-  ooids
-  vertical burrows
-  fenestral fabrics
-  bioclasts
-  hardground and/or ferruginous crusts
-  intraformational reworking
-  dolomite bed+ iron impregnation
-  thin lamination
-  microbial lamination
-  sequence boundary
-  scale: 5 m



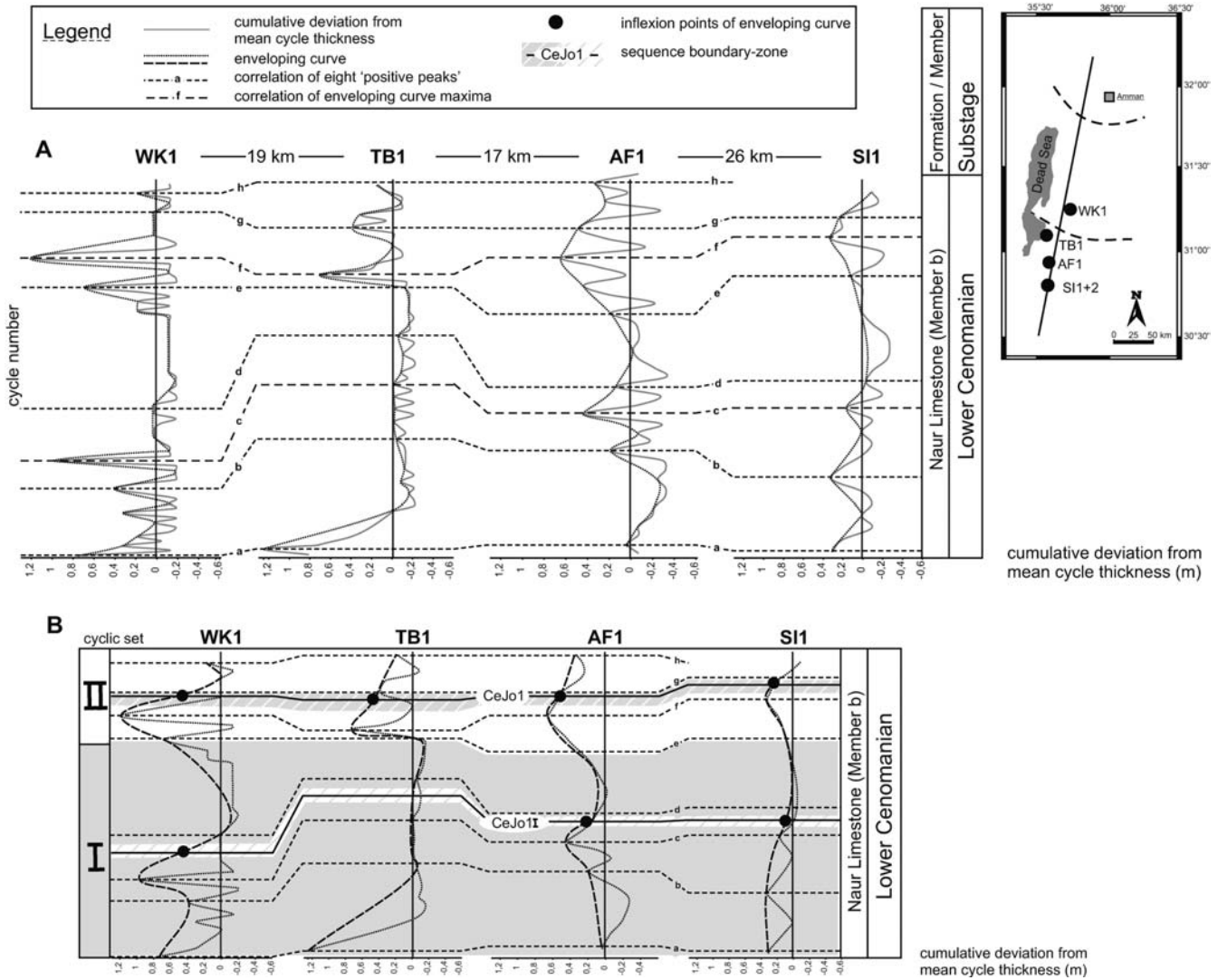


Fig. 10 a The accommodation plots of sections AF1 and SI1+2 (see Fig. 9) are compared with two additional curves from a southern and a central section (TB1, WK1; compare map). Eight peaks of positive deviation from the mean cycle thickness are correlated (thin dashed lines), while the two main peaks are accentuated (peaks 'c' and 'f'). A higher-ranking trend in accommodation fluctuation is created by graphic correlation (dotted, enveloping curve). **b** A second enveloping curve is created (thick

dashed line; graphic correlation of the eight main positive peaks 'a' to 'h') and these higher-ranking accommodation trends are compared. Two cyclic sets (I+II) can be subdivided, each containing a rising accommodation trend, a maximum, and decreasing accommodation. Furthermore, each cyclic set includes four 'positive accommodation peaks', one inflexion point of the second enveloping curve (above the two accommodation maxima), within the zone of a corresponding sequence boundary (CeJo1, CeJo1I)

and/or reworking, as well as by diagenetic alteration and compaction (e.g. Grötsch 1996). Subtidal cycles that do not contain a peritidal unit and which are separated by a rapid deepening on top of each cycle occur less fre-

quently. After Osleger (1991) and Goldhammer et al. (1993), they can indicate a lack of shoreline progradation. To sum up, the occurrence of small-scaled cycles, and the uniform subdivision into cyclic sets over tens of kilometres on the platform, implies allocyclic control. In this case the most likely allocyclic controlling factor is eustasy (compare Goldhammer et al. 1993; Strasser et al. 1999; Grötsch 1996). Moreover, previous authors discussed higher-frequency cycles as a result of orbitally-driven mechanisms (e.g. Strasser 1994; Balog et al. 1997; Gale et al. 2002). Eustatic oscillations triggered by orbital mechanisms thus can produce cycles with duration of about 400, 100, 41 ky or 23 to 19 ky (e.g. Fischer 1991). Although, the lack of age control inhibits the calculation

Fig. 9 Two detailed lower Cenomanian sub-sections of the southern study area (AF 1, SI1+2; compare map), with cm to m-scale shallowing-up cycles are illustrated. The cumulative deviation from the mean cycle thickness of both sections has been plotted against the cycle number. These curves are interpreted as accommodation plots. Comparisons of both curves result in seven partly correlatable positive deviation-peaks (dashed lines, 'a'-'g'), while the uppermost peak ('h') is only observed in the plot of section AF1. Scale bars of the section logs in metres. For extensive explanation see text

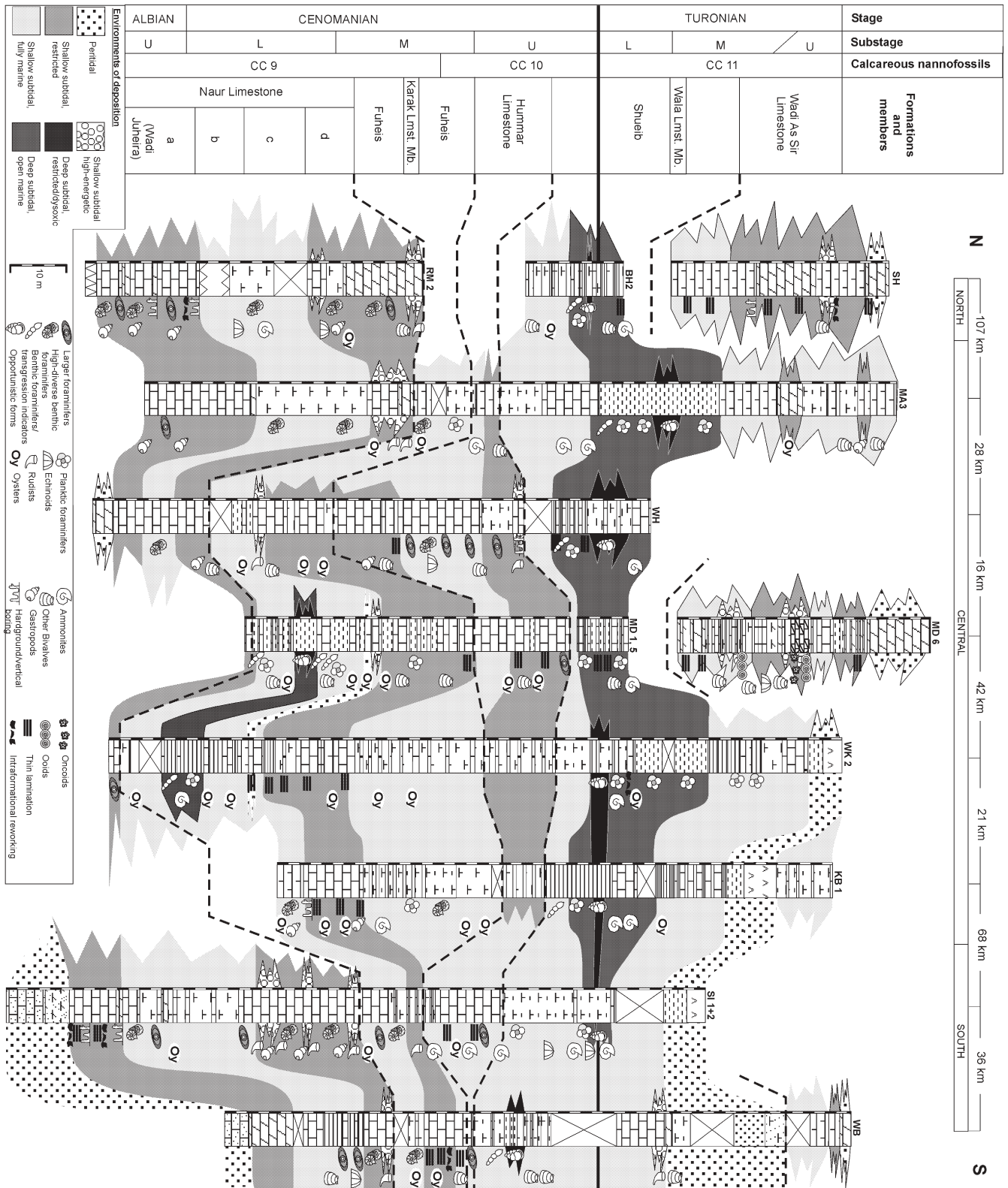


Fig. 11 The temporal and spatial distribution of six environments of deposition is illustrated, based on twelve sections within a north to south correlation. These data are integrated into a stratigraphic scheme (left column, dashed lines; compare Powell 1989 and

Schulze et al. 2003). The datum line coincides with the Cenomanian/Turonian-boundary. Indicative fossils and textures are marked on the right side of each section

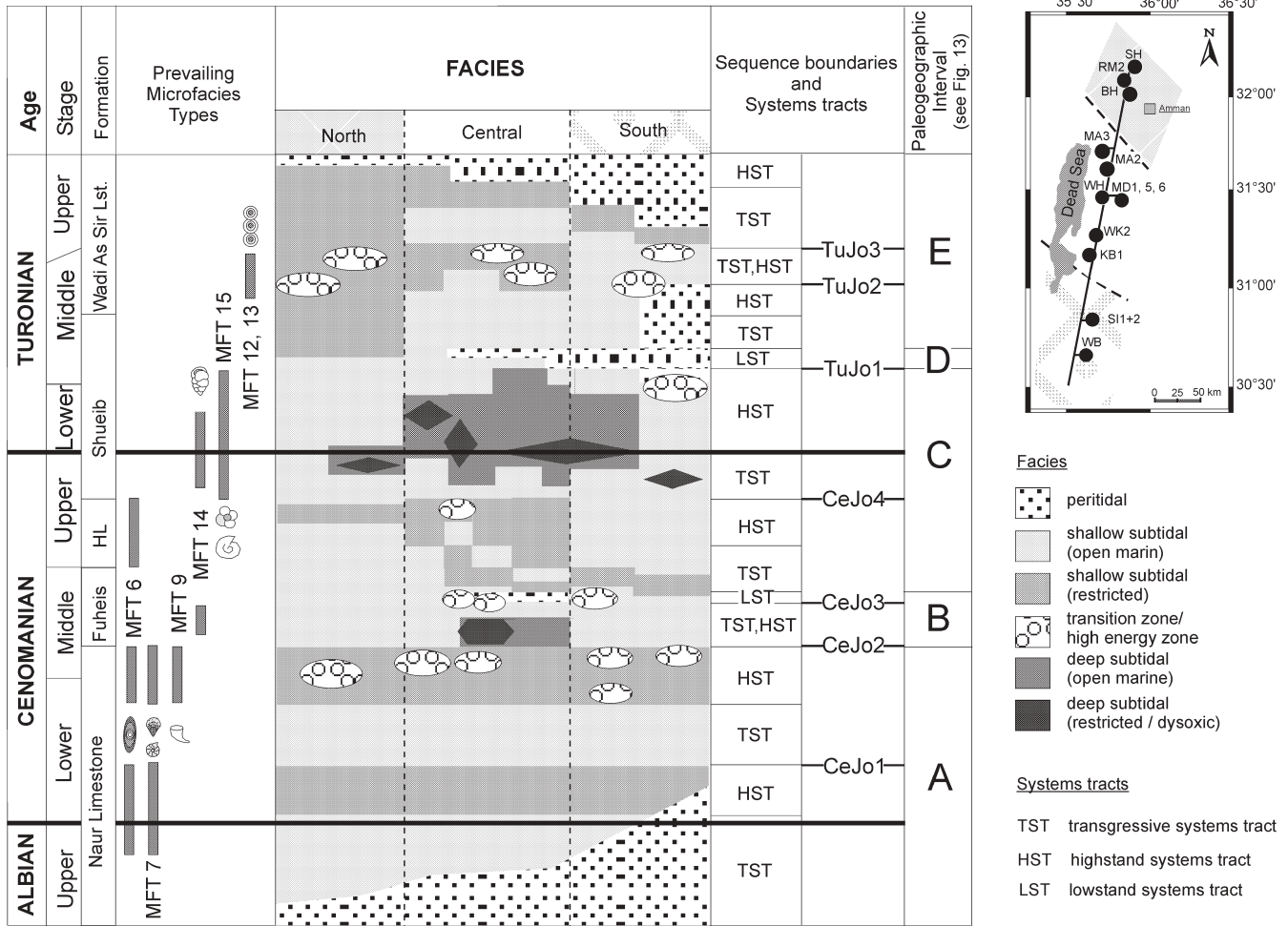


Fig. 12 Generalised lateral and vertical facies distribution based on the sections and successions in Fig. 11 (and indicated on the map) is illustrated in the middle column. The stratigraphic range of the investigated formations is indicated in left columns, as well as the most characteristic microfacies types (MFT) for Cenomanian/

Turonian-boundary interval, and for facies belts on the Turonian platform. The facies distribution model is compared to the sequence stratigraphic scheme of the study area (right column; compare Schulze et al. 2003). Five intervals of platform development and paleogeographic situations (A–E) are illustrated. For explanation of abbreviations and signatures see legend in Figs. 11 and 12

of our cycle durations, the orbitally control on Cenomanian to Turonian cyclicities in Jordan is favoured.

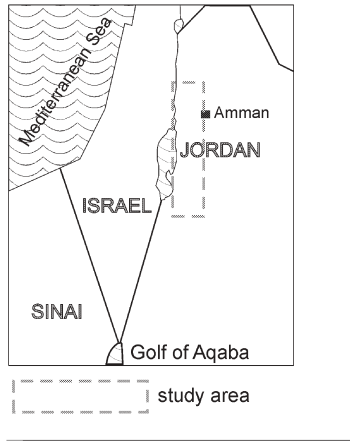
Lateral and vertical distribution of facies belts

Apart from facies changes within Cenomanian and Turonian higher-frequency cycles, the lateral facies distribution was also investigated. Based on these data, the study area has been subdivided into a northern, a central, and a southern part (Figs. 2, 11 and 12).

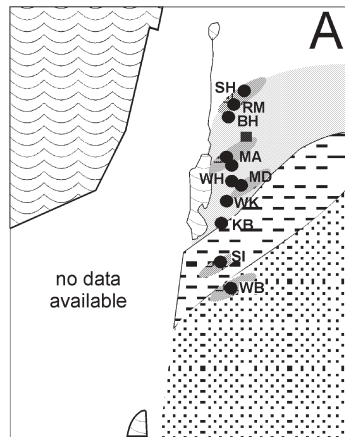
The northern part

Distinctive facies features of the northern sections are restricted and higher-energy shallow subtidal environments within Cenomanian and Turonian limestone and dolostone successions (Naur Formation, members b and

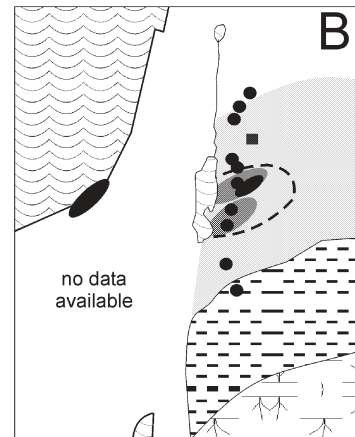
d; Hummar Formation; Wadi As Sir Formation; Fig. 11). Moreover, certain microfacies types (MFT's) characterise the upper Albian to upper Cenomanian platform carbonates: wackestones and packstones with abundant gastropods, or monospecific larger agglutinated or alveolinid foraminifers, alternating with wackestones and packstones with an abundant and highly diverse benthic and planktic biota (e.g. foraminifers, green algae, bivalves, echinoids). Rudist patch reefs (MFT 9) mainly represent the higher-energy zones. The same environments are represented by different microfacies types during the Turonian: deep subtidal, open marine environments are observed in uppermost Cenomanian and lower Turonian deposits, indicated by bituminous, partly thinly laminated marls and limestones that contain high amounts of planktic foraminifers and abundant ammonites. Dysoxic conditions (section BH2, Fig. 11) are locally reflected by an opportunistic benthic faunal association.



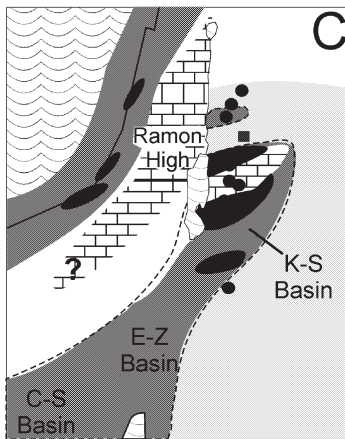
Pre-CeJo2 HST
(middle Cenomanian)



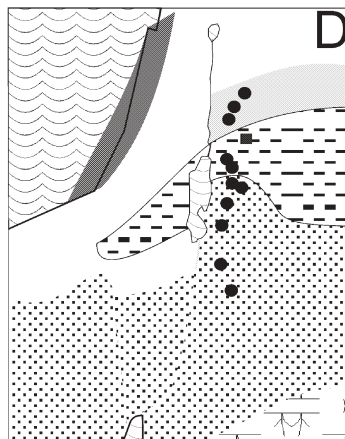
Pre-CeJo3 TST
(middle Cenomanian)



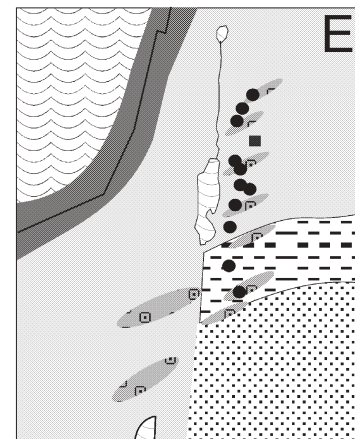
Pre-TuJo1 TST/HST
(upper Cenomanian/
lower Turonian)



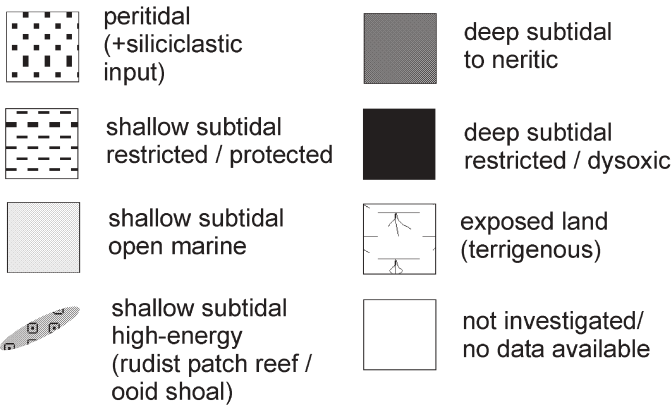
Post-TuJo2 LST
(middle Turonian)



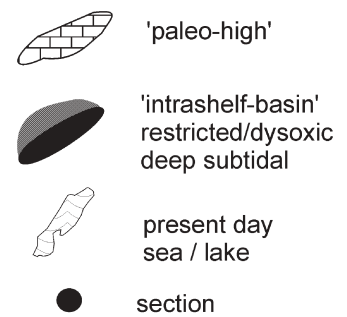
Pre-TuJo3 TST/HST
(upper Turonian)



Facies belts



Structural elements



The central part

Deposits of the described open marine deep subtidal environment characterise middle Cenomanian successions of the area of Wadi Mujib and Wadi Al Karak (Figs. 2 and 11) and the Cenomanian/Turonian (CT)-boundary interval of all central sections as well. The onset of the second deepening is indicated by clayey marls and a benthic foraminifer assemblage, consisting of *Lenticulina* sp., *Dentalina* sp. or *Fronicularia* sp. Restricted deep subtidal environments with local dysoxic conditions are observed during middle Cenomanian times exclusively in the area of Wadi Mujib, but within the CT-boundary interval it developed in several central locations (section MD1; Figs. 2 and 11). The restriction is indicated by bituminous shales, thin lamination, organic-rich mudstones and an assemblage of abundant opportunistic smaller benthic foraminifers (*Praebulimina* spp., *Gabonita* spp.). Peritidal environments locally occur during middle Cenomanian times and from Wadi Mujib southward, during late Turonian times (claystones and evaporites).

The southern part

The vertical changes of facies belts are similar to those of the northern study area during early Cenomanian and late Turonian times. Nevertheless, some differences, such as a general thinning of facies belts towards the south or an increase of deposition in peritidal environments highlight the proximity to the continent. Within the CT-boundary interval, a transgressive facies and occasionally deeper-water and dysoxic environmental conditions are reflected by claystones, and benthic foraminifers (section SII+2, Fig. 11). Locally, the same can be recognized during late Cenomanian times (section WB, Fig. 11). Siltstones and sandstones are equivalent to the late Turonian peritidal facies of central sections.

Fig. 13 The map in the upper left corner constitutes the basemap for the paleogeographic reconstructions/map **a** to **e**. Paleogeographic reconstructions for a part of the Levant Platform (see Fig. 1a) are illustrated for five intervals (**a–e**, see Fig. 12). The distribution of facies belts and major structural elements during one or two chosen systems tracts of each time slice (TST, HST, LST; compare Fig. 12) is reconstructed for the study area. Data of the adjacent shelf areas (Israel, Egypt) have been considered, if available. Note that the post-Cretaceous shift along a sinistral transform fault (Quennell 1956) was reversed for the reconstructions. **a** Uniform facies distribution; prevailing shallow subtidal facies belts; general shallowing towards the south, **b** Interval of local subsidence; basins with dysoxic conditions in Israel and Jordan (central study area), **c** Interval with basin inversion (Sinai, Israel, Jordan/Wadi Mujib area) and increased subsidence: North Sinai and North Israel, Central-Sinai-Basin (C–S), Eshet-Zenifim-Basin (E–Z) and Karak-Silla-Basin (K–S); Locally dysoxic conditions (Israel, west-central Jordan), **d** Extended sea-level lowstand characterised by prevailing peritidal environments; increased terrigenous input towards the south, **e** Uniform facies distribution; prevailing shallow subtidal environments; high-energy areas (ooid shoals) characterise TST's and HST's in Sinai and the study area

Paleogeography

The north to south correlation of facies belts integrated into the sequence stratigraphic framework (Fig. 12), allow to reconstruct the paleogeographic conditions of certain time intervals and sedimentary sequences (Fig. 13) and therefore the major steps of platform development. Five of such intervals are identified, and compared with those from adjacent shelf areas (Israel: Buchbinder et al. 2000; Lipson-Benitah et al. 1990 and Egypt: Kuss et al. 2000 and Bauer et al. 2002; Fig. 13).

Interval A

This time interval contains upper Albian to middle Cenomanian deposits of the Naur Formation (Fig. 12). Compared to the early Albian terrigenous environments of the underlying Kurnub Group that indicate an extensive sea-level lowstand (Powell 1989), during interval A a transgression from NW to SE is reflected by a discontinuity and by a distinct increase of siliciclastics from north to south (Fig. 12; compare Powell 1989). Moreover, comparisons with eustatic sea-level fluctuations (Haq et al. 1987) and with regional facies and sequence stratigraphic models (Bauer et al. 2002; Sharland et al. 2001; Buchbinder et al. 2000; Lewy and Avni 1988; compare also Schulze et al. 2003) emphasise two major sequences that occur within interval A. Except for local rudist patch reefs, the lower Cenomanian platform shows an uniform structuring. The paleogeographic reconstruction (Fig. 13a) illustrates the facies distribution during the lower/middle Cenomanian HST. Northern and central parts of the study area are covered by an open marine, shallow subtidal facies belt, while the south is more influenced by restricted shallow subtidal or even peritidal conditions.

Interval B

Interval B includes middle Cenomanian deposits of the Fuheis Formation (Fig. 12). Deposits of the early interval B reflect predominantly open shallow subtidal conditions and point to a transgression. The following HST is characterised by restricted shallow subtidal to intertidal environments. In the central study area, near Wadi Mujib and Wadi AL Karak, the TST includes deeper-water shales and faunas and dysoxic conditions are occasionally observed at Wadi Mujib during this transgressive phase. Such a deeper-water and occasionally dysoxic facies is also described from west Israel for middle Cenomanian times (Lipson-Benitah et al. 1990, Fig. 13b). Moreover, in some central sections the HST succession is overlain by a peritidal facies, probably indicating a relative sea-level lowstand.

Interval C

Interval C spans the upper middle Cenomanian to lower middle Turonian (Fuheis, Hummar, Shueib Formation), and consists of two sedimentary sequences (Fig. 12). In the north and south, the lower part of interval C is predominated by open, shallow subtidal facies but central sections reflect dominantly restricted conditions. Moreover, a transgression that affected the entire shelf segment is reflected by open marine shallow subtidal environments in the upper part of interval C (Shueib Formation). The greatest thickness of open deep subtidal deposits is observed from central sections of the Wadi Abu Kusheiba area and near Wadi Al Karak. Furthermore, deeper subtidal deposits of restricted and dysoxic environments locally occur in the uppermost Cenomanian, but within the central study area they straddle the CT-boundary (Figs. 11 and 12). Sections near Wadi Mujib do not reflect such a 'basinal' setting in the upper part of interval C, but show characteristics of an elevated area instead (condensation). Comparable structures on the inner shelf are described from adjacent shelf areas in Israel and Egypt (Fig. 13c). During the latest interval C, a late HST is documented by shallow open subtidal facies belts in northern and southern sections, while in the central study area, the open marine deeper-water facies persisted and underlines the basinal structure of that region. Former higher-energy conditions and peritidal environments are additionally reflected in the southernmost sections, reflecting the general shallowing trend towards the continent.

Interval D

This interval contains middle Turonian deposits of the upper Shueib Formation (Fig. 12). Distinct facies changes took place during interval D. Northward prograding supratidal deposits and terrigenous input reflect a major sea-level lowstand (Fig. 13d). North of Wadi Mujib these environments interfinger with restricted shallow subtidal facies belts (Fig. 12). The lithological differences again mark a basinal structure in the central study area (claystones, evaporites) and the proximity to the continent in the south (siltstones, sandstones).

Interval E

Interval E comprises middle and upper Turonian deposits of the Wadi As Sir Formation and is subdivided into three sedimentary sequences (Fig. 12). Open shallow marine environments dominate the early interval E, while deposits of a high-energy facies (ooid shoals) characterise the transgressive phases of the middle part of this interval (Fig. 13e). In contrast, the latest interval E reflects prevailing restricted shallow subtidal conditions, whereas the shallowing of the shelf towards the south is indicated by increasing peritidal conditions and terrigenous input. Apart from this distal/proximal trend, the equal facies

distribution is comparable to the conditions during early Cenomanian times (interval A; Fig. 13a).

Discussion

A little pronounced paleorelief on the inner shelf and broad subtidal to peritidal facies belts are described from all mentioned shelf areas during the early Cenomanian and during the late Turonian. The development of a basinal facies in the area of Wadi Mujib and Wadi Al Karak during the middle Cenomanian (interval B; Fig. 13b) coincides on the one hand with the recorded dysoxic basinal deposition in Israel and with extensional movements described from Sinai, that resulted in locally increasing subsidence related to 'halfgrabens' (Bauer et al. 2003) during late Cenomanian times. A coeval increase of subsidence in the central Sinai (C-S-Basin), in central and south Israel (E-Z-Basin), and in the central and southern study area (K-S-Basin, compare Kuss et al. 2003) resulted in the development of larger basins, which were probably connected to each other (Fig. 13c). On the other hand, graben inversion during the CT-boundary interval is described by Bauer et al. (2003) from Sinai, and simultaneous uplift or decreased subsidence is observed in the area of Wadi Mujib in Jordan. These 'paleo-highs' seem to belong to the uplifted area in Israel (Makhtesh Ramon; Buchbinder et al. 2000). Exposure at these locations is assumed by e.g. Bartov et al. (1980), Lewy and Avni (1988), Bauer et al. (2003) for Egypt and Israel, but it is not recorded in the Wadi Mujib area in Jordan. The local organic-rich, dysoxic facies within the basins of Israel (Lipson-Benitah et al. 1990) and west-central Jordan (Schulze et al. 2003) occur in latest Cenomanian and early Turonian times and may characterise the depocentres of the basinal structures, while the proximity to the mentioned elevated areas has probably provided the development of small-scale and restricted sub-basins (Fig. 13c). The connection between late Cenomanian to Turonian tectonic movements on shelf areas of Egypt and the Near East, and a probable initial Syrian Arc deformation is discussed by e.g. Kuss et al. (2000), Bauer et al. (2003) and Schulze et al. (2003), though the main deformation phase is described from the Santonian (Bosworth et al. 1999). Furthermore, Gvirtzman and Garfunkel (1998) postulated a magmatic swell in southern Israel, westward of Wadi Abu Kusheiba and Wadi Mujib (Jordan, Fig. 2) during early Cretaceous times. This paleo-high coincides well with the reconstructed structures in Egypt, Israel and Jordan on the upper Cretaceous shelf.

Conclusions

A facies scheme, including fifteen microfacies types (MFTs) and eight environments of deposition, is defined for upper Albian to Turonian shelf deposits of west-central Jordan. Peritidal to open marine, shallow subtidal environments prevailed during lower Cenomanian and upper

Turonian times. Deeper subtidal and occasionally restricted, dysoxic facies conditions prevailed in the central study area during the middle Cenomanian (Wadi Mujib; Fuheis Formation), and in the entire study area during the upper Cenomanian to the middle Turonian (Shueib Formation). Moreover, comparison with a facies scheme of Sinai/Egypt reveals a more terrigenous influenced coastal marine facies belt for the Sinai, but a very similar organisation of the subtidal facies belt. The restricted deeper subtidal facies that reflect small-scale basinal deposition under dysoxic conditions on the inner shelf in west-central Jordan (and Israel), is not observed in Sinai.

Analyses of Cenomanian carbonate cycles in Jordan, imply high-frequency facies and accommodation changes, while major cyclic patterns are correlatable over large parts of the study area and suggest, after integration into the sequence stratigraphic scheme of the study area, an additional lower Cenomanian sequence boundary (CeJo 11). The results of accommodation analyses imply control by allocyclic mechanisms (eustasy).

Basinal deposition and extensional movements during the pre-CeJo transgression (middle Cenomanian), are described from Jordan and the adjacent areas. Deeper-water conditions also occur in Jordan, Sinai and Israel during pre-TuJo1 TST and HST. Locally, in NW Israel, in the areas of Wadi Abu Kusheiba, Wadi Al Karak, and in the southern study area, dysoxic conditions are indicated. Therefore, we assume an eastward extension of the basins in Sinai (Central-Sinai-Basin) and Israel (Eshet-Zenifim-Basin) towards west-central Jordan (Karak-Silla-Basin). Moreover, tectonic inversion is postulated in the Wadi Mujib area for the same time slice, resulting in a paleo-high that is comparable to a time equivalent structure in Israel (Ramon High). The conjunction of these major structural elements underlines the similar shelf organisation and development of these parts of the Levant Platform.

Acknowledgements Funding was provided by the German Science Foundation (Deutsche Forschungsgemeinschaft Ku 642/16–2). We thank the National Resources Authority (NRA), Amman/Jordan for the valuable logistic support in Jordan, and A. Gharaibeh (NRA, Amman) for his help in the field. Moreover, we have to point out that A. M. M. Morsi and A. M. Bassiouni (both Ain Shams University, Cairo/Egypt) helped to classify the ostracodes, and Z. Lewy (Geological Survey, Jerusalem/Israel) identified the ammonites. We also thank R. Bätzel for the preparation of the thin sections as well as M. Bachmann, J. Bauer, S. Lüning and C. Scheibner (all Bremen University), for fruitful discussions and comments. Special thanks go to Prof. Dr. A. Freiwald, who has attended to the publication of this study with extensive endurance and to Prof. Dr. A. Strasser and Prof. Dr. P. Wright for their constructive comments of the manuscript.

References

- Al-Rifaiy IA, Cherif OH (1987) Biostratigraphic aspects and regional correlation of some Cenomanian/Turonian exposures in Jordan. *Géol Méditerranéenne* XIV (3):181–193
- Al-Rifaiy IA, Cherif OH, El-Bakri BA (1993) Upper Cretaceous foraminiferal biostratigraphy and paleobathymetry of the Al-Baqa area, north of Amman (Jordan). *J Afric Earth Sci* 17(3):343–357
- Arthur MA, Schlanger SO, Jenkyns HC (1987) The Cenomanian-Turonian Oceanic Anoxic Event, II. Palaeoceanographic controls on organic-matter production and preservation. In: Brooks J, Fleets AJ (eds) Marine petroleum source rocks. *Geol Soc Lond Spec Publ* 26:401–420
- Bacelle L, Bosellini A (1965) Diagrammi per la stima visiva della composizione percentuale nelle rocce sedimentarie. *Sci Geol Paleont* 1:59–62
- Bachmann M, Kuss J (1998) The Middle Cretaceous carbonate ramp of the northern Sinai: sequence stratigraphy and facies distribution. In: Wright VP, Burchette TP (eds) Carbonate ramps. *Geol Soc Lond Spec Publ* 149:253–280
- Balog A, Haas J, Read F, Coruh C (1997) Shallow marine record of orbitally forced cyclicity in a Late Triassic carbonate platform, Hungary. *J Sediment Res* 67(4):661–675
- Bandel K, Geys JF (1985) Regular echinoids in the Upper Cretaceous of the Hashemite Kingdom of Jordan. *Ann Soc Géol Nord C IV*:97–115
- Bartov Y, Lewy Z, Steinitz G, Zak I (1980) Mesozoic and Tertiary stratigraphy, paleogeography and structural history of the southern Israel. *Isr J Earth Sci* 29:114–139
- Bathurst RGC (1966) Boring algae, micritic envelopes, and lithification of molluscan biosparites. *Geol J* 5:15–32
- Bauer J, Marzouk A, Steuber T, Kuss J (2001) Lithostratigraphy and biostratigraphy of the Cenomanian–Santonian strata of Sinai, Egypt. *Cretaceous Res* 22:497–526
- Bauer J, Kuss J, Steuber T (2002) Platform environments, microfacies and systems tracts of the upper Cenomanian-lower Santonian of Sinai, Egypt. *Facies* 47:1–26
- Bauer J, Kuss J, Steuber T (2003) Sequence architecture and carbonate platform configuration (Late Cenomanian-Santonian), Sinai, Egypt. *Sedimentology* 50(3):387–414
- Boss SK, Rasmussen KA (1995) Misuse of Fischer plots as sea-level curves. *Geology* 23(3):221–224
- Bosworth W, Guiraud R, Kessler LG (1999) Late Cretaceous (ca. 84 Ma) compressive deformation of the stable platform of northeast Africa (Egypt): far-field stress effects of the “Santonian event,” and origin of the Syrian arc deformation belt. *Geology* 27(7):633–636
- Buchbinder B, Benjamini C, Lipson-Benitah S (2000) Sequence development of Late Cenomanian–Turonian carbonate ramps, platforms and basins in Israel. *Cretaceous Res* 21:813–843
- Burchette TP, Wright VP (1992) Carbonate ramp depositional systems. *Sediment Geol* 79:3–57
- Caron M (1985) Cretaceous planktic foraminifera. In: Bolli HM, Saunders JB, Perch-Nielsen K (eds) Plankton stratigraphy. Cambridge University Press, Cambridge, pp 17–86
- Dunham RJ (1962) Classification of carbonate rocks according to depositional texture. In: Ham WE (ed) Classification of carbonate rocks. *Am Assoc Geol Mem* 1:108–121
- Fischer AG (1964) The Lofer cyclothems of the alpine Triassic. *Kansas Geol Surv Bull* 169:107–149
- Fischer AG (1991) Orbital cyclicity in Mesozoic strata. In: Einsele G, Ricken W, Seilacher A (eds) Cycles and events in stratigraphy. Springer, Berlin Heidelberg New York, pp 48–62
- Flügel E (1982) Microfacies analyses of limestones. Berlin, 633 pp
- Folk RL (1962) Petrography and origin of Silurian Rochester and McKenzies Shales, Morgan County, West Virginia. *J Sediment Petrol* 32(3):539–578
- Freund R, Raab M (1969) Lower Turonian ammonites from Israel. *Spec Pap Palaeontol* 4:83
- Gale AS, Hardenbol J, Hathway B, Kennedy WJ, Young JR, Phansalkar V (2002) Global correlation of Cenomanian (Upper Cretaceous) sequences: evidence for Milankovitch control on sea level. *Geology* 30(4):291–294
- Garber RA, Friedmann GM, Nissenbaum A (1981) Concentric aragonitic ooids from the Dead Sea. *J Sediment Petrol* 51(2):455–458
- Ginsburg RN (1971) Landward movement of carbonate mud: new model for regressive cycles in carbonate (abstract). *Am Assoc Petroleum Geol Ann Meet* 55:340

- Goldhammer RK, Lehmann PJ, Dunn PA (1993) The origin of high-frequency platform carbonate cycles and third-order sequences (Lower Ordovician El Paso Gp, West Texas): constraints from outcrop data and stratigraphic modeling. *J Sediment Petrol* 63(3):318–359
- Gradstein FM, Agterberg FP, Ogg JG, Hardenbol J, Van Veen P, Thierry J, Huang Z (1995) A Triassic, Jurassic and Cretaceous time scale. In: Berggren WA, Kent DV, Aubry M-P, Hardenbol J (eds) *Geochronology, time scales and global stratigraphic correlation*. SEPM Spec Publ 54:95–126
- Grötsch J (1996) Cycle stacking and long-term sea-level history in the Lower Cretaceous (Gavrovo Platform, NW Greece). *J Sediment Res* 66:723–736
- Gvirtzman Z, Garfunkel Z (1998) Birth and decay of an intracontinental magmatic swell: Early Cretaceous tectonics of southern Israel. *Tectonics* 17(3):441–457
- Hamaoui M, Saint-Marc P (1970) Microfaunes et microfaciès du Cénomaniens du proche-orient. *Bull Centre Rech Pau-SNPA* 4(2):257–352
- Haq B, Hardenbol J, Vail PR (1987) Chronology of fluctuating sea levels since the Triassic. *Science* 235:1156–1167
- Hardenbol J, Thierry J, Farley MB, Jacquin T, De Graciansky P-C, Vail PR (1998) Mesozoic and Cenozoic sequence chronostratigraphic framework of European basins. In: De Graciansky P-C, Hardenbol J, Jacquin T, Vail PR (eds) *Mesozoic and Cenozoic sequence stratigraphy of European basins*. SEPM Spec Publ 60:343–360
- Koch W (1968) Zur Mikropaläontologie und Biostratigraphie der Oberkreide und des Alttertiärs von Jordanien. *Geol Jahrb* 85:627–668
- Kuss J, Westerhold T, Groß U, Bauer J, Lüning S (2000) Mapping of Late Cretaceous stratigraphic sequences along a Syrian Arc uplift—examples from the Areif el Naqa, Eastern Sinai. Middle East Research Center, Ain Shams University. *Earth Sci Ser* 14:171–191
- Kuss J, Bassiouni A, Bauer J, Bachmann M, Marzouk A, Scheibner C, Schulze F (2003) Cretaceous-Paleogene sequence stratigraphy of the Levant Platform (Egypt, Sinai, Jordan). In: Gili E, Negra H, Skelton P (eds) *North African cretaceous carbonate platform systems*. *Nato Sci Ser* 28:171–187
- Lewy Z (1989) Correlation of lithostratigraphic units in the upper Judea Group (Late Cenomanian – Late Coniacian) in Israel. *Isr J Earth Sci* 38:37–43
- Lewy Z (1990) Transgressions, regressions and relative sea-level changes on the Cretaceous shelf of Israel and adjacent countries. A critical evaluation of Cretaceous global sea-level correlations. *Paleoceanography* 5(4):619–637
- Lewy Z, Avni Y (1988) Omission surfaces in the Judea Group, Makhtesh ramon region southern Israel, and their paleogeographic significance. *Isr J Earth Sci* 37:105–113
- Lipson-Benitah S, Flexer A, Rosenfeld A, Honigstein A, Conway B, Eris H (1990) Dysoxic sedimentation in the Cenomanian—Turonian Daliyya Formation, Israel. *AAPG, Stud Geol* 30:27–39
- Masri M (1963) Report on the geology of the Amman-Zerqa area, Central water authority, (unpublished), Amman, Jordan, 74 pp
- Morsi A-MM, Bauer J (2001) Cenomanian ostracode faunas from Sinai Peninsula, Egypt. *Revue Paléobiol* 20(2):377–414
- Mustafa H, Bandel K (1992) Gastropods from lagoonal limestones in the Upper Cretaceous of Jordan. *Neues Jahrb Geol Paläont Abh* 185(3):349–375
- Nederbragt AJ (1991) Late Cretaceous biostratigraphy and development of Heterohelicidae (planktic foraminifers). *Micropaleontology* 37:329–372
- Osleger D (1991) Subtidal carbonate cycles: implications for allocyclic vs. Autocyclic controls. *Geology* 19:917–920
- Pasquier J-B, Strasser A (1997) Platform-to-basin correlation by high-resolution sequence stratigraphy and cyclostratigraphy (Berriasian, Switzerland and France). *Sedimentology* 44:1071–1092
- Perch-Nielsen K (1985) Mesozoic calcareous nannofossils. In: Bolli HM, Saunders JB, Perch-Nielsen K (eds) *Plankton stratigraphy*. Cambridge University Press, Cambridge, pp 329–554
- Philip J, Babinot J-F, Tronchetti G, Fourcade E, Ricou L-E, Guiraud R, Bellion Y, Herbin J-P, Combes P-J, Cornee J-J, Dercourt J (2000) Late Cenomanian. In: Dercourt J, Gaetani M, Vrielynck B, Barrier E, Biju-Duval B, Brunet MF, Cadet JP, Crasquin S, Sandulescu M (eds) *Atlas Peri-Tethys palaeogeographical maps*, Map 14, CCGM/CGMW, Paris
- Powell JH (1989) Stratigraphy and sedimentation of the Phanerozoic rocks in Central and South Jordan. Pt. B: Kurnub, Ajlun and Belqa groups. *NRA Geol Bull* 11:130 pp
- Pratt BR, James NP, Cowan CA (1992) Peritidal Carbonates. In: Walker RG, James NP (eds) *Facies models*. Response to sea level change. *Geol Assoc Can*, pp 303–322
- Quennell AM (1951) The geology and mineral resources of (former) Transjordan. *Colon Geol Min Res* 2:85–115
- Quennell A (1956) The structural and geomorphic evolution of the Dead Sea Rift. *Q J Geol Soc Lond* 114:1–24
- Sadler PM, Osleger DA, Montanez IP (1993) On the labelling, length and objective basis of Fisher Plots. *J Sediment Petrol* 63:360–368
- Saint-Marc P (1974) Etude stratigraphique et micropaléontologique de l'Albien, du Cenomanien et du Turonien du Liban. Notes et memoires sur le moyen-orient, 13, Museum National d' Histoire Naturelle, Paris, 298 pp
- Sarg JF (1988) Carbonate sequence stratigraphy. In: Wilgus CK, Hastings BS, Kendall CGSC, Posamentier HW, Ross CA, Van Wagoner JC (eds) *Sea-level changes: an integrated approach*. SEPM Spec Publ 42:155–182
- Schröder R, Neumann M (1985) Les grandes foraminifères du Cretacé Moyen de la region mediterrannee. *Geobios mem spec* 7:160 pp
- Senowbari-Daryan B, Kuss J (1992) Anomuren-Koprolithen aus der Kreide von Ägypten. *Mitt Geol-Paläont Inst Univ Hamburg* 73:129–157
- Sharland PR, Archer R, Casey DM, Davies RB, Hall SH, Heward AP, Horbury AD, Simmons MD (2001) Arabian Plate sequence stratigraphy. *Geo Arabia Spec Publ* 2, Bahrain, 371 pp
- Schulze F, Lewy Z, Kuss J, Gharaibeh A (2003) Cenomanian–Turonian carbonate platform deposits in west-central Jordan. *Int J Earth Sci* 92(4):641–660
- Schulze F, Marzouk AM, Bassiouni MAA, Kuss J (2004) The upper Albian to Turonian carbonate platform succession of west central Jordan—stratigraphy and crisis. *Cretaceous Res* 25(5):709–737
- Sissingh W (1977) Biostratigraphy of calcareous nannofossils. *Geol Mijnbouw* 56:37–65
- Strasser A (1991) Lagoonal-peritidal sequences in carbonate environments: autocyclic and allocyclic processes. In: Einsele G, Ricken W, Seilacher A (eds) *Cycles and events in stratigraphy*. Springer, Berlin Heidelberg New York, pp 709–721
- Strasser A (1994) Milankovitch cyclicity and high-resolution sequence stratigraphy in lagoonal-peritidal carbonates (Upper Tithonian-Lower Berriasian, French Jura Mountains). In: de Boer PL, Smith DG (eds) *Orbital forcing and cyclic sequences*. *Spec Publ Int Assoc Sediment* 19:285–301
- Strasser A, Pittet B, Hillgärtner H, Pasquier J-B (1999) Depositional sequences in shallow carbonate-dominated sedimentary systems: concepts for a high-resolution analysis. *Sediment Geol* 128:201–221
- Stampfli GM, Borel G, Cavazza W, Mosar J, Ziegler PA (2001) The Paleotectonic Atlas of the Peritethyan Domain. European geophysical society, CD-ROM, Electronic Publishing and Consulting, Berlin
- Tucker ME, Wright VP (1990) *Carbonate sedimentology*. Blackwell Sci Publ, Oxford, 482 pp
- Vail PR, Audemard SA, Bowman SA, Eisner PN, Perez-Cruz C (1991) The stratigraphic signatures of tectonics, eustasy and sedimentology—an overview. In: Einsele G, Seilacher A (eds) *Cycles and events in stratigraphy*. Springer, Berlin Heidelberg New York, pp 617–662

- Van Wagoner JC, Posamentier HW, Mitchum RM, Vail PR, Sarg JF, Loutit TS, Hardenbol J (1988) An overview of the fundamentals of sequence stratigraphy and key definitions. In: Wilgus CK, Hastings BS, Kendall CG St C, Posamentier HW, Ross CA, Van Wagoner JC (eds) Sea-level changes: an integrated approach. SEPM Spec Publ 42:39–45
- Weidich KF, Al-Harithi T (1990) Agglutinated foraminifera from the Albian and Cenomanian of Jordan. In: Hemleben C, Kaminski MA, Kuhnt W, Scott DB (eds) Paleocology, biostratigraphy, paleoceanography and taxonomy of agglutinated foraminifera. NATO ASI 327(C), Kluwer Academic Publishers, Dordrecht, pp 587–609
- Wilson JA (1975) Carbonate facies in geologic history. Springer, Berlin Heidelberg New York, 471 pp